PALEOCEANOGRAPHY, VOL. 14, NO. 2, PAGES 118-134, APRIL 1999

The isotopic composition of diatom-bound nitrogen in Southern Ocean sediments

Daniel M. Sigman,[1,2] Mark A. Altabet,[3] Roger Francois,[1] Daniel C. McCorkle,[1] and Jean-Francois Gaillard[4]

Abstract. Treatment of diatom microfossils from Southern Ocean sediments with hot perchloric acid leaves a "diatom-bound" N fraction which is 0-4‰ lower in $\delta^{15}N$ than the bulk sediment, typically 3‰ lower in recent Antarctic diatom ooze. Results from Southern Ocean surface sediments indicate that early diagenetic changes in bulk sediment N content and $\delta^{15}N$ are not reflected in diatom-bound N, suggesting that diatom-bound N is physically protected from early diagenesis by the microfossil matrix. A meridional transect of multicores from the Indian sector of the Southern Ocean shows a northward increase in the $\delta^{15}N$ of diatom-bound N, suggesting that diatom-bound $\delta^{15}N$, like bulk sedimentary $\delta^{15}N$, varies with nitrate utilization in the overlying surface waters. The $\delta^{15}N$ of diatom-bound N is 3-4‰ higher in glacial age Antarctic sediments than in Holocene sediments, supporting the hypothesis, previously based on bulk sediment $\delta^{15}N$, that nitrate utilization in the surface Antarctic was higher during the last ice age. While there are important uncertainties, the inferred range of utilization changes could potentially explain the entire ~80 ppm amplitude of observed glacial/interglacial variations in atmospheric CO_2.

1. Introduction

Field and laboratory studies show that isotopic fractionation during nitrate uptake links the degree of nitrate consumption by phytoplankton to the isotopic composition of nitrate, suspended particulate N, and the sinking N flux in marine systems [*Wada and Hattori*, 1978; *Wada*, 1980; *Altabet and McCarthy*, 1985; *Altabet et al.*, 1991; *Francois et al.*, 1992; *Nakatsuka et al.*, 1992; *Altabet and Francois*, 1994a; *Montoya and McCarthy*, 1995; *Pennock et al.*, 1996; *Wu et al.*, 1997; *Waser et al.*, 1998]. In the case of a finite nitrate pool the preferential uptake of ^{14}N nitrate relative to ^{15}N nitrate by phytoplankton causes the $\delta^{15}N$ of nitrate to increase as a function of "nitrate utilization," the fraction of the initial nitrate supply which is consumed ($\delta^{15}N$, in permil versus atmospheric N_2 = $\{[(^{15}N/^{14}N)_{sample}/(^{15}N/^{14}N)_{atm}] - 1\}*1000$). Because nitrate is typically the ultimate N source in nutrient-replete marine ecosystems, progressive nitrate utilization causes a parallel increase in the $\delta^{15}N$ of newly formed biomass N.

In the Southern Ocean the nitrate utilization/N isotope link has been most explicitly studied through isotopic measurements of nitrate, which have demonstrated that the $\delta^{15}N$ variations of nitrate in the surface layer are dominated by a quantitatively consistent correlation with nitrate utilization [*Sigman*, 1997]. The $\delta^{15}N$ of nitrate increases into the surface layer, in concert with the decrease in nitrate concentration due to nitrate uptake by phytoplankton [*Sigman et al.*, 1997; D.M. Sigman et al., The $\delta^{15}N$ of nitrate in the Southern Ocean, 2, Nitrate supply and uptake in surface waters, submitted to *Global Biogeochem. Cycles*, 1998b, hereinafter referred to as Sigman et al., submitted manuscript, 1998b]. In addition, the $\delta^{15}N$ of surface nitrate increases toward the north in the Southern Ocean, in parallel with the decrease in surface nitrate concentration toward the north (Sigman et al., submitted manuscript, 1998b). Sediment trap data and surface sediment data demonstrate that this nitrate utilization/$\delta^{15}N$ relationship is recorded in open ocean sediments, albeit with a 2-5‰ diagenetic increase during incorporation into the sediment record [*Francois et al.*, 1992; *Altabet and Francois*, 1994a; *Farrell et al.*, 1995]. On this basis, downcore variations in sedimentary $\delta^{15}N$ may provide information on the history of nitrate utilization in the Southern Ocean. While there are some important complexities in such interpretations for the Subantarctic Zone (north of the modern Polar Frontal Zone), we would expect the nitrate utilization/$\delta^{15}N$ relationship of the Antarctic Zone (south of the Polar Front) to persist through oceanographic changes (D.M. Sigman et al., The $\delta^{15}N$ of nitrate in the Southern Ocean, 1, Nitrogen cycling and circulation in the ocean interior, submitted to *J. Geophys. Res.*, 1998a, hereinafter referred to as Sigman et al., submitted manuscript, 1998a; Sigman et al., submitted manuscript, 1998b).

Sediment cores from the Antarctic record a change in bulk sediment nitrogen isotopic composition at the last glacial/interglacial transition. The $\delta^{15}N$ of last glacial sediments is 1-4‰ higher than the $\delta^{15}N$ of Holocene sediments [*Francois et al.*, 1992, 1997]. This glacial/interglacial bulk sediment $\delta^{15}N$ change has been hypothesized to record a higher degree of nitrate utilization in Antarctic surface waters during the last ice age [*Francois et al.*, 1992, 1997]. This change would have had far-reaching implications for the circulation of the Southern Ocean and for observed glacial/interglacial changes in the atmospheric concentration of carbon dioxide [*Knox and McElroy*, 1984; *Sarmiento and Toggweiler*, 1984; *Siegenthaler and*

[1]Woods Hole Oceanographic Institution, Woods Hole, Massachusetts.
[2]Now at Department of Geosciences, Princeton University, Princeton, New Jersey.
[3]Center for Marine Science and Technology, University of Massachusetts, New Bedford.
[4]Department of Geological Sciences, Northwestern University, Evanston, Illinois.

Paper number 1998PA900018.
0883-8305/99/1998PA900018$12.00

Wenk, 1984; *Broecker and Peng*, 1987, 1989; *Keir*, 1988, 1990; *Sarmiento and Orr*, 1991].

One concern about this interpretation involves the potential effect of diagenetic and sedimentary processes on bulk sediment $\delta^{15}N$. Given the significant $\delta^{15}N$ increase associated with the incorporation of sinking organic N into surface sediments [*Altabet and Francois*, 1994a] and evidence for variability in this isotopic enrichment as a function of the degree of preservation [*Sachs*, 1997], diagenetic or other sedimentary changes may be responsible for the isotopic difference between last glacial and Holocene sediments in Antarctic sediment cores. The impact of diagenesis on paleoceanographic records can be assessed and overcome by isolating sedimentary organic material which is either protected from diagenesis or are not isotopically affected by it [e.g., *Hayes et al.*, 1989; *Jasper and Hayes*, 1990; *Sachs*, 1997].

Shemesh et al. [1993] pioneered the use of diatom microfossils to overcome the uncertainties of bulk sediment carbon and nitrogen isotopic composition. The premise of this approach is that organic matter resides within the hydrated silica matrix of diatom microfossils, that this organic matter was incorporated into the microfossils by the living diatoms, and that the organic matter is physically protected by the opal matrix from bacterial decomposition, both within the water column and at the seafloor. In their analytical procedure, diatom-bound organic matter is isolated by physical separation of the diatom microfossil fraction from the other components of the sediment, followed by wet chemical oxidation to remove any organic matter on the microfossil surface. The remaining organic matter, presumably within the microfossils, is converted to gas for mass spectrometry by combustion of the surface-oxidized diatom microfossil material.

Southern Ocean diatom-bound organic carbon isotopic records generated in this way show a pattern similar to that of bulk sediment $\delta^{13}C_{org}$ records, with lower $\delta^{13}C$ values during ice ages [*Singer and Shemesh*, 1995]. However, diatom-bound $\delta^{15}N$ was also found to be lower in glacial-age sediments than in Holocene sediments [*Shemesh et al.*, 1993], which is in the opposite sense to the $\delta^{15}N$ change observed in bulk sediments [*Francois et al.*, 1992, 1993, 1997]. The results of *Shemesh et al.* [1993] indicate that diatom $\delta^{15}N$ is 9-11‰ in Holocene sediments, which is ≥5‰ higher than bulk sediment $\delta^{15}N$ and ≥8‰ higher than the $\delta^{15}N$ of the N sinking flux [*Wada et al.*, 1987; Sigman et al., submitted manuscript, 1998b; M. Altabet and R. Francois, unpublished data, 1998].

In this study we report N isotope measurements of diatom-bound N from recent and glacial age Southern Ocean sediments. These results support the use of diatom-bound N as a paleoceanographic tool. In contrast to the downcore results of *Shemesh et al.* [1993], we find that the $\delta^{15}N$ of diatom-bound organic N is 3-4‰ higher in glacial sediments than in Holocene sediments, in qualitative agreement with the downcore change which occurs in bulk sedimentary $\delta^{15}N$ [*Francois et al.*, 1992, 1997].

2. Materials

We have studied (1) a multicore profile from the Antarctic Zone in the west Pacific sector of the Southern Ocean, (2) a north-south transect of multicore profiles from the central Indian sector, and (3) two paleoceanographic-scale cores from the Antarctic, one in the Atlantic sector and one in the central Indian sector (Figure 1 and Table 1). The multicore NBP 96-4-2 MC 4 was collected from the Antarctic Zone of the west Pacific sector (64°S, 170°E) during the Joint Global Ocean Flux Study Southern Ocean sediment trap site survey cruise of the R/V *Nathaniel B. Palmer* in September 1996. A depth profile in one subcore is used to study the relationship between bulk sediment and diatom microfossil-bound N during the course of early diagenesis. The meridional transect of multicores from the Indian sector was collected during the ANTARES 1 cruise of the R/V *Marion Dufresne* in March-May 1993 [*Gaillard*, 1997]. We use this transect to test for a northward increase in diatom $\delta^{15}N$, which should occur if diatom $\delta^{15}N$ varies with nitrate utilization in the Southern Ocean surface, in analogy to the observed north-south gradients in nitrate $\delta^{15}N$ and bulk sediment $\delta^{15}N$ [*Francois et al.*, 1992; *Altabet and Francois*, 1994a; Sigman et al., submitted manuscript, 1998b]. Two cores, gravity core AII 107-22 GGC from the Atlantic Antarctic (55°S, 3°W, 2768 m depth) and piston core MD 84-552 from the Indian Antarctic (55°S, 74°E, 2230 m) provide records of diatom $\delta^{15}N$ across the last glacial/interglacial transition. Both cores are from the modern Antarctic Zone and have planktonic foraminiferal oxygen isotope stratigraphies [*Keigwin and Boyle*, 1989; L.D. Labeyrie, personal communication, 1996].

3. Methods

To isolate diatom-bound N, we use (1) physical separation steps to isolate the diatom microfossil fraction from the bulk sediment and (2) chemical oxidation of the diatom microfossil fraction to remove labile organic matter on the exterior of the microfossils. The physical separation methods follow the sieving and settling approach of *Shemesh et al.* [1988] with the addition of two steps: (1) a 10 μm sieving step to aid with clay removal and (2) a heavy liquid step to remove detrital grains and clays. We use an oxidation procedure similar to that of *Shemesh et al.* [1993] and *Singer and Shemesh* [1995], which employs an oxidizing acid at 70°C. However, we use concentrated (72%) perchloric acid alone, rather than the nitric acid/perchloric acid mixture used by *Shemesh et al.* [1993], since nitric acid represents a potential source of contamination for N isotope work. *Sigman* [1997] reports the complete protocol for the isolation of diatom-bound N and additional data on the application of the physical and chemical steps of the isolation protocol to a number of sediment standards from the Southern Ocean.

The isotopic and N content analyses were performed on a Europa Roboprep elemental analyzer on line with a Finnigan MAT 251 stable isotope ratio mass spectrometer. Isotopic values are reported in permil (‰) units versus laboratory air N_2, which is checked for consistency using several types of calibrated lab standards, including dried solutions of 6-aminocaproic acid, glycine, potassium nitrate, and ammonium sulfate. Ammonium sulfate standard solution pipetted onto an acidified glass fiber disk typically yields a standard deviation of 0.15‰. Isotopic measurements of diatom-bound N are less precise because they have a low N content. The standard deviation for this type of sample is ~0.3‰ or better for analysis during a single day. Our long-term precision is somewhat worse,

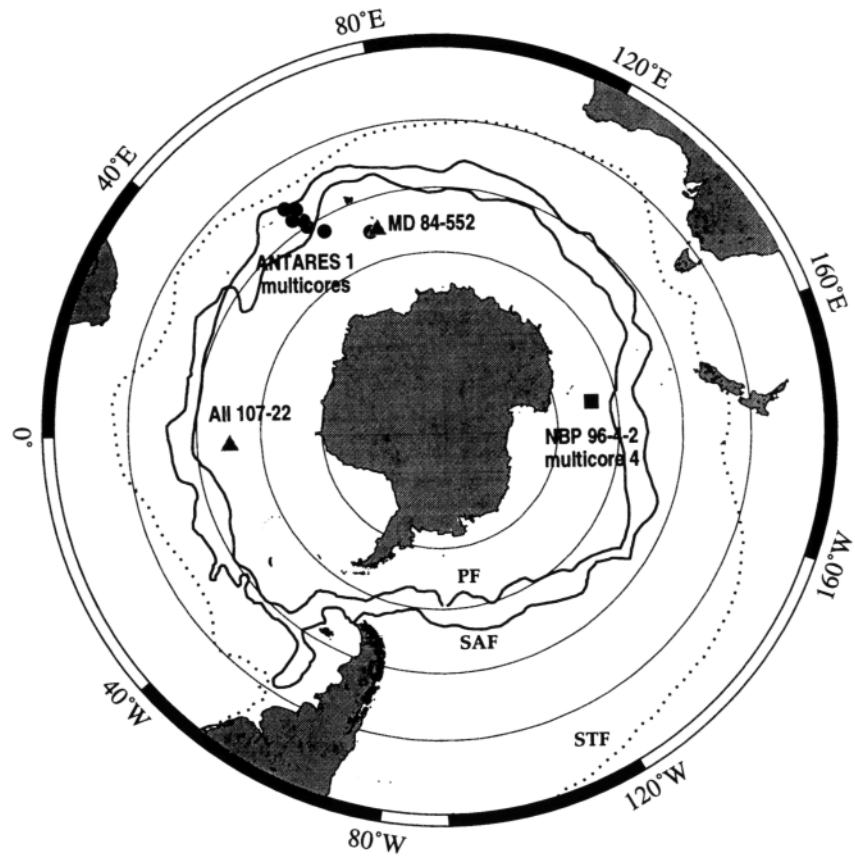

Figure 1. Map view of the Southern Ocean cores used in this study. NBP 96-4-2 MC 4 (solid square) is from a multicore in diatom ooze from the Antarctic Zone in the west Pacific sector. This core is used to study the effect of early diagenesis on diatom-bound N. The ANTARES 1 multicores (solid circles) from the central Indian sector provide a meridional transect across the Polar Frontal Zone, which is used to investigate the role of nitrate utilization in the isotopic variation of diatom-bound N. All 107-22 GGC, a gravity core from the Atlantic sector of the Antarctic Zone, and MD 84-552, a piston core from the Indian sector of the Antarctic Zone, are used to generate diatom-bound $\delta^{15}N$ records back through the Last Glacial Maximum (solid triangles). The Polar Front (PF, more southern solid line) separates the Antarctic Zone to the south from the Polar Frontal Zone to the north. The Subantarctic Front (SAF, more northern solid line) separates the Polar Frontal Zone to the south from the Subantarctic Zone to the north. The Subtropical Front (STF, dotted line) separates the Subantarctic Zone to the south from the subtropical gyre to the north. Frontal positions are from *Orsi et al.* [1995].

with a standard deviation of ≤0.5‰, probably because of changes in the sediment combustion conditions. N content, measured by integration of the major ion beam, has a long term relative standard deviation of 5-10% for diatom-bound N samples.

To evaluate the effects of the chemical oxidation step, subsamples of a diatomaceous sediment standard (NBP 96-4-3 MC 6, 14-20 cm, 62°S, 170°E) were oxidized with concentrated perchloric acid at 70°C for different lengths of time (1, 6, and 20 hours). Because the sediment is a very pure diatomaceous ooze, the physical separation step was not necessary to purify the diatom fraction from this sediment standard, as verified by the physical separation and treatment of a subsample. After 1 hour of oxidation the diatom microfossils show a 3‰ decrease in $\delta^{15}N$ and a decrease in N content of 5 μmol N g^{-1} sediment (Figure 2a). Continued oxidation (with renewal of the perchloric acid) has no further effect on either N content or $\delta^{15}N$. The reproducibility of the isolated N fraction through 20 hours of perchloric acid treatment suggests either that the surviving N is physically isolated within the diatom microfossils or that its chemical structure makes it recalcitrant to the chemical oxidant over tens of hours. Physical protection seems more likely since one would expect a spectrum of reactivities for surviving N that is accessible to the oxidant, which would lead to gradual changes in N content and $\delta^{15}N$ over the course of the experiment.

An oxidation time-course experiment with bleach as the chemical oxidant shows a continued decrease in N content

Table 1. Sample Locations

Site Name	Purpose	Location
NBP 96-4-2 multicore 4	shallow depth profile	64°S, 170°E
ANTARES 1 multicores:		
KTB 5	meridional transect	55°S, 72°E
KTB 6	meridional transect	52°S, 61°E
KTB 13	meridional transect	50°S, 58°E
KTB 11	meridional transect	49°S, 58°E
KTB 16	meridional transect	48°S, 56°E
KTB 19	meridional transect	47°S, 58°E
KTB 21	meridional transect	46°S, 56°E
All 107-22 (gravity core)	paleoceanographic record	55°S, 3°W
MD 84-552 (piston core)	paleoceanographic record	55°S, 74°E

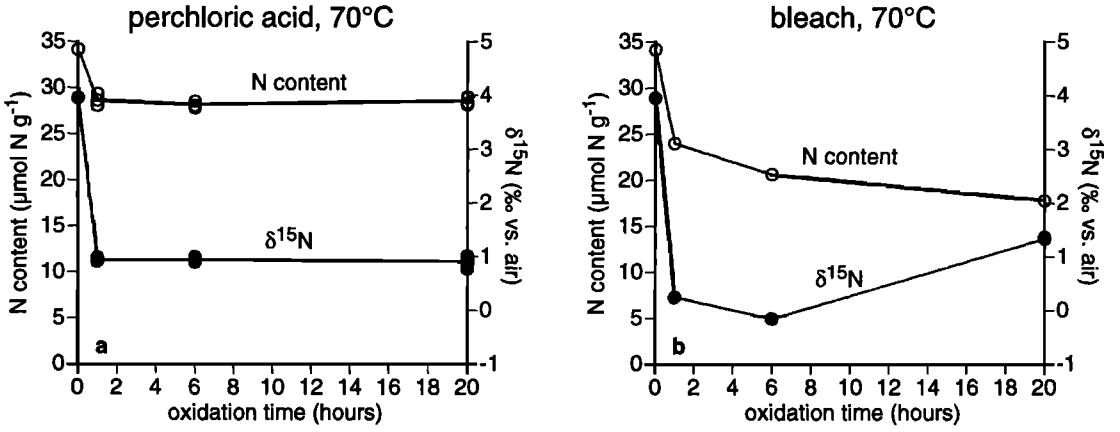

Figure 2. Time course of $\delta^{15}N$ (solid circles) and N content (open circles) in a diatom ooze sediment standard (NBP 96-4-3 MC 6, 62°S, 170°E) for treatment with (a) concentrated perchloric acid at 70°C (as in the standard protocol) and (b) bleach at 70°C. New reagent was added at the 1 and 6 hour time steps. Replicate analyses are shown, and solid lines connect the analysis means. The changes observed throughout the bleach treatment are probably due to etching and dissolution of the diatom microfossils in this basic solution.

throughout the experiment, with lower values than observed with perchloric acid treatment, and the $\delta^{15}N$ of the remaining N also varies with oxidation time (Figure 2b). We suspect that the isotopic variations and continued N loss are due to the loss of diatom-bound N during progressive etching and leaching of the microfossils over the course of the treatment because opal is soluble in alkaline solutions such as bleach, which has a *p*H of ≥11.5. Despite the continued N loss and isotopic variation, which make bleach a poor choice for the chemical oxidant, the diatom-bound $\delta^{15}N$ values are within ~1‰ of the value which results from treatment with perchloric acid.

Other oxidative treatments give similar isotopic results (Table 2). Treatment with a 1/1 30% H_2O_2/50% HCl mixture yields a $\delta^{15}N$ value which is ~0.5‰ higher than results from the standard perchloric acid treatment. Carrying out both the perchloric and peroxide treatments in either order yields $\delta^{15}N$ values which are close to the standard perchloric acid treatment alone. This suggests that the perchloric acid treatment cleans the diatom surfaces more completely than does the H_2O_2/HCl solution. Oxidation using either boiling or fuming perchloric acid yields $\delta^{15}N$ values which are ~0.5‰ lower than in the standard perchloric acid treatment, which is carried out at 70°C. In addition, these hotter perchloric acid treatments result in a lower N content in the treated diatom microfossils. These results may indicate that perchloric acid treatment at 70°C fails to remove a small remaining fraction of the physically vulnerable N which is isotopically enriched because of diagenesis. Alternatively, the difference may be due to slight isotopic alteration associated with organic N breakdown and release during boiling with perchloric acid. The data reported in section 4 are for diatom samples cleaned with concentrated perchloric acid at 70°C.

Table 2. Chemical Treatments of a Diatom Ooze

Treatment	$\delta^{15}N$, ‰ versus air	N Content,[a] μmol N g^{-1}
Untreated	4.0	34.1
72% H_4CLO_4, 70°C	1.0	27.6
1/1 30% H_2O_2/50% HCl, 70°C[b]	1.6	30.4
1/1 30% H_2O_2/50% HCl, 70°C, followed by 72% H_4CLO_4, 70°C	1.1	22.3
72% H_4CLO_4, 70°C, followed by 1/1 30% H_2O_2/50% HCl, 70°C	0.9	22.8
36% H_4CLO_4 (initial), boiled 2 hours	0.5	20.5
36% H_4CLO_4 (initial), boiled to fuming, fuming 1 hour	0.4	20.5
Bleach, 70°C, 1 hour	0.2	24.0
Bleach, 70°C, 6 hours	-0.2	20.6
Bleach, 70°C, 20 hours	1.4	17.8
1/1 HNO_3/72% H_4ClO_4, 70°C, 20 hours, 3 DI rinses, filtration	3.9	156.5
1/1 HNO_3/72% H_4ClO_4, 70°C, 20 hours, 8 DI rinses, filtration	3.1	131.5
Deionized water, 70°C, 20 hours	3.4	48.5

The sediment standard is from 14-20 cm depth in NBP 96-4-3 multicore 6 (64°S, 170°E).

[a] No correction is made here for the weight losses which occur during these treatments (see text).

[b] The 1/1 30% H_2O_2/50% HCl treatment was carried out for an hour past the time when the peroxide was consumed (when bubbling stopped).

The decrease in $\delta^{15}N$ which results from our oxidative treatments is in contrast to the very high $\delta^{15}N$ values (9-12‰) which resulted from the 1/1 nitric/perchloric acid oxidation of Holocene, Antarctic diatomaceous sediments in the study of *Shemesh et al.* [1993], although no direct bulk/diatom $\delta^{15}N$ comparison was presented in that study. We have used the nitric/perchloric cleaning protocol of *Shemesh et al.* [1993] on our diatomaceous sediment standard, rinsing and filtering the cleaned diatoms repeatedly in an attempt to remove all readily desorbable nitric acid (Table 2). However, the treated diatom fraction has a N content which is several fold higher than the original bulk sediment. This suggests that N from the nitric acid is incorporated into the microfossil material or its organic constituents, raising doubts about the significance of the diatom $\delta^{15}N$ data of *Shemesh et al.* [1993]. Repeated rinses with deionized water gradually lowered the N content of nitric-treated samples (Table 2), suggesting that at least part of the contaminant N is only loosely bound. However, eight repetitions of deionized water addition, centrifugation, and decantation followed by filtration and rinsing with >600 mL deionized

Table 3. C/N of Diatom-Bound Organic Matter

Sediment	Location	C/N (molar)
NBP 96-4-2 MC4, 4.25 cm	64°S, 170°E	6.2
NBP 96-4-2 MC4, 8.5 cm	64°S, 170°E	6.3
NBP 96-4-2 MC4, 9.5 cm	64°S, 170°E	6.3
ANTARES 1 KTB 5, 9-10 cm	55°S, 72°E	6.9
ANTARES 1 KTB 6, 9-10 cm	52°S, 61°E	5.6
ANTARES 1 KTB 13, 9-10 cm	50°S, 58°E	5.8
ANTARES 1 KBE 3, 9-10 cm	49°S, 58°E	6.5
ANTARES 1 KTB 11, 9-10 cm	49°S, 58°E	6.8
ANTARES 1 KTB 16, 9-10 cm	48°S, 56°E	6.3
ANTARES 1 KTB 19, 9-10 cm	47°S, 58°E	5.0
ANTARES 1 KTB 21, 9-10 cm	46°S, 56°E	6.2

water left the treated diatoms with high levels of contaminant N (Table 2).

An ~25% weight loss occurs during treatment of the diatom microfossils with perchloric acid. This weight loss appears to occur early in the treatment and is not repeated upon subsequent treatment. Most of this weight loss is also observed upon heating of our bulk diatomaceous sediment standard overnight at 70°C in deionized water. Treatment with hot deionized water also causes an ~35% increase in N content (Table 2), as is expected from a 25% decrease in sediment weight which does not liberate sedimentary N. The decrease in weight may be due to opal dissolution and dehydration or to the dissolution of hygroscopic authigenic phases. In other studies, chemical treatment of sediments has been observed to increase the organic matter content, suggesting that sediment weight loss is a common result of chemical treatment (J. Whelan, personal communication, 1997).

The molar C/N ratio of the diatom-bound organic matter tends to range between 5 and 7, showing no consistent correlation with $\delta^{15}N$ (Table 3). This range of C/N ratios, along with results from pyrolysis/gas chromatography/mass spectrometry [*Sigman*, 1997] and amino acid analysis (J. Brandes and P. Schafer, unpublished results, 1998), suggest that the microfossil-bound organic matter is largely proteinaceous. In addition, fluorescence microscopy indicates that diatom-bound organic matter is distinct from the diagenetically altered, amorphous organic matter which is external to the diatom microfossils and disseminated throughout the sediment [*Sigman*, 1997]. In contrast to the disseminated organic matter, the diatom-bound organic matter has a component which fluoresces intensely when excited with 450-490 nm light, indicating that the diatom-bound organic matter is relatively unaltered [*Senftle et al.*, 1993]. Despite the expected lability of such fresh organic matter it survives the perchloric acid treatment, suggesting that it is physically protected by the microfossils. *Swift and Wheeler* [1992] report that an oxidative treatment of cultured diatom microfossils yields a proteinaceous material which is internal to the microfossils, supporting a diatom-native origin for the organic matter within sedimentary diatom microfossils.

4. Results and Interpretation

4.1. Depth Variations in Antarctic Sediments

In multicore NBP 96-4-2 MC 4 from the Pacific Antarctic, bulk sediment N content decreases with depth (Figure 3, open circles), as is commonly observed in open ocean sediments [e.g., *Muller*, 1977]. However, the concentration of diatom-bound N is constant with depth (Figure 3, solid circles). Dia-

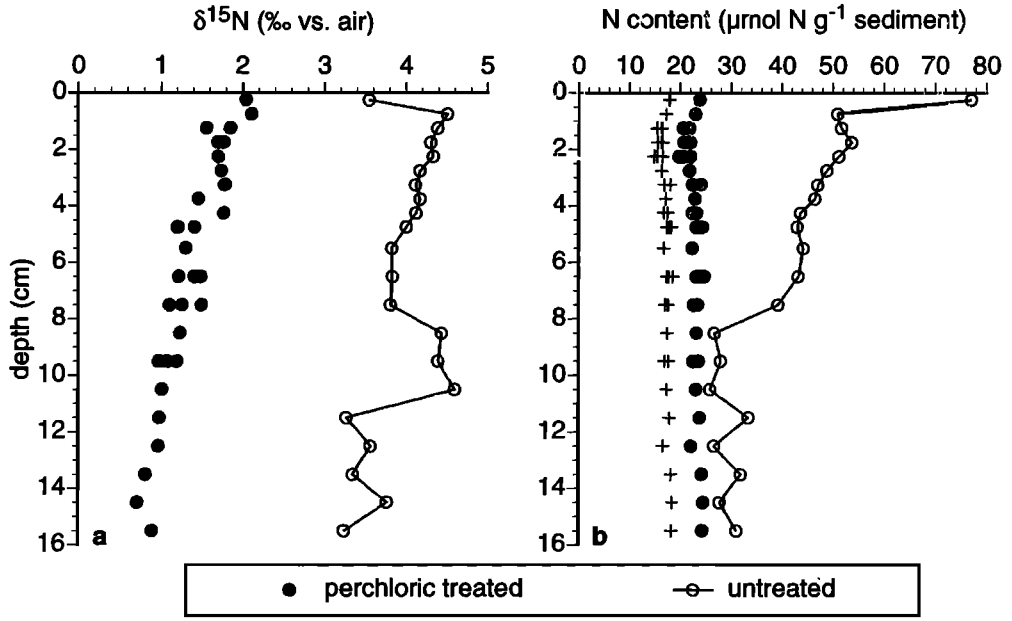

Figure 3. Depth profiles in a multicore in diatom ooze (NBP 96-4-2 MC 4, Antarctic Zone, west Pacific sector, 64°S, 170°E) of the (a) $\delta^{15}N$ and (b) N content before (open circles) and after (solid circles) treatment with perchloric acid at 70°C. Replicate analyses are shown, and solid lines connect the means of the bulk sediment analyses. The crosses in Figure 3b indicate the calculated N content of the cleaned diatom material, corrected for the 25% sediment weight loss, which does not appear to remove diatom-bound N (see text). These sediments are almost entirely diatomaceous, so no physical separation steps were performed, allowing for a more direct comparison of N content between the treated and untreated material. Application of the physical separation protocol to one subsample had no discernible effect on the measured diatom-bound $\delta^{15}N$.

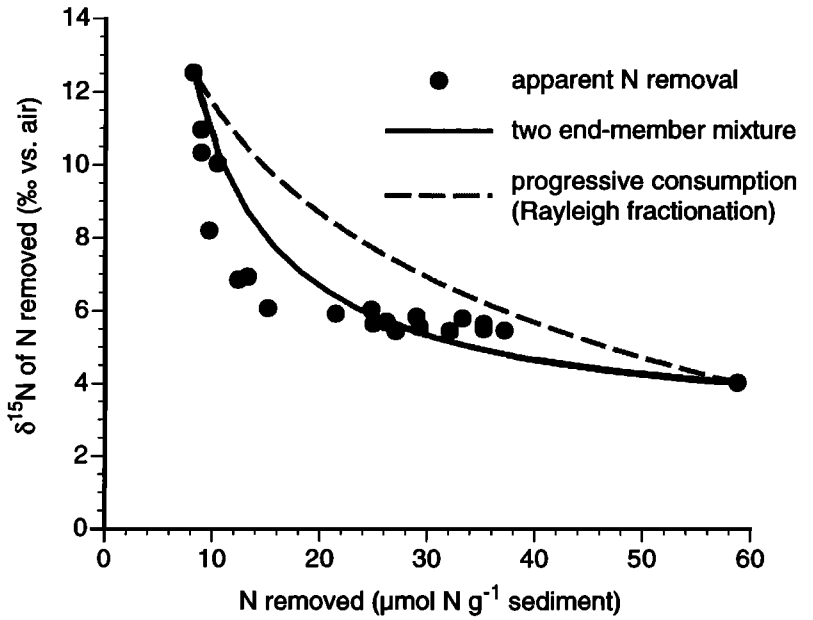

Figure 4. Estimates of the $\delta^{15}N$ of the N lost from the sediments of NBP 96-4-2 MC 4 during treatment with perchloric acid, plotted versus the estimated amount of N lost, based on the N content and $\delta^{15}N$ data for the bulk sediment and perchloric acid-treated sediment, with N content corrected for sediment weight loss during the treatment (crosses in Figure 3b). At least some of the N lost during perchloric oxidation has been involved in diagenesis, making these estimates useful for understanding diagenetic effects. The data show more curvature than is predicted by a model of constant fractionation during degradation (the Rayleigh model, dashed line), so that the data are better fit by a model of two N pools with different $\delta^{15}N$ values and different rates of degradation (solid line). The Rayleigh fractionation model is calculated using the uppermost sediment sample, which has the most N removed, as the starting point and using an isotope effect of 4.5‰, which causes the Rayleigh fractionation model to fit the sample with the least N removed. The two-pool model is a mixing curve between two N pools, with the assumed end-members being the samples with the most and least N removed. While the data are not very well predicted by the two-pool model, the highly curved trend of the data appears to support a model of multiple N pools which are degraded on different time scales. A key assumptions in our comparison is that all sediment samples evolved from the same initial composition.

tom-bound N appears to be a major fraction of sedimentary N in these diatomaceous sediments, implying that physical protection plays an important role in sedimentary N preservation [*Muller*, 1977; *Mayer*, 1994].

The $\delta^{15}N$ of the bulk diatomaceous sediment is 3-5‰, which is 2-4‰ higher than the apparent mean annual sinking flux $\delta^{15}N$ in this sector of the Antarctic (0-1‰ based on a nitrate isotope balance [*Sigman*, 1997] and 0.5‰ based on measurements from a moored sediment trap (M. Altabet and R. Francois, unpublished results, 1998). This difference is consistent with comparisons of sediment trap and surface sediment $\delta^{15}N$ from other open ocean regions, which have demonstrated a diagenetic enrichment of 2-5‰ in bulk sediments [*Altabet and Francois*, 1994a]. The diatom-bound $\delta^{15}N$ is 0.8-2.0‰ in MC 4, and Holocene diatom-bound $\delta^{15}N$ from all other Antarctic sites in this study is similarly between 0.5 and 2.0‰. The ~3‰ difference between diatom-bound and bulk sediment $\delta^{15}N$ is qualitatively consistent with the hypothesis that diatom-bound N does not undergo the 2-5‰ increase in $\delta^{15}N$ associated with diagenesis of bulk sediment on the seafloor.

Downcore changes in the $\delta^{15}N$ of bulk sediment in MC 4 coincide with changes in N content. The uppermost section of the core, which includes a "fluff layer" at the sediment/water interface, is characterized by high N content and a ~1‰ lower $\delta^{15}N$ than the underlying sediment (Figure 3). Similar patterns have been observed for bulk sediment $\delta^{15}N$ profiles from the equatorial Pacific and appear to reflect the incorporation of the recent biogenic rain into the sediment column (M. Altabet, unpublished results, 1998). Another shift in bulk sediment $\delta^{15}N$ occurs at 8-12 cm depth and coincides with a downcore decrease in bulk sediment N content (Figure 3).

These depth variations in bulk sediment $\delta^{15}N$ are not matched by variations in diatom-bound $\delta^{15}N$ (Figure 3a). This is consistent with the interpretation that the bulk sediment variations are diagenetic and that these diagenetic changes do not affect diatom-bound N. Both bulk and diatom-bound N show a gradual ~1‰ decrease in $\delta^{15}N$ with depth (Figure 3a). This change may indicate a longer time scale diagenetic effect on the diatom-bound N, or it may record a long-term change in the isotopic composition of the sinking flux being incorporated into the sediment column at this site. The lack of downcore change in diatom-bound N content supports the latter alternative.

While the difference in N content between bulk sediment and diatom-bound N decreases with depth, the $\delta^{15}N$ difference between bulk and diatom-bound N is ~3‰ down the entire multicore profile (Figure 3). This implies that the $\delta^{15}N$ of the organic N removed by chemical oxidation increases with depth, becoming enriched as the size of the labile organic N pool decreases [*Macko et al.*, 1993]. The amount of N removed during perchloric acid treatment and its $\delta^{15}N$ can be estimated by mass balance using the N content and $\delta^{15}N$ data (Figure 4). Our estimates are complicated somewhat by the ~25% decrease in sediment weight which occurs during the perchloric acid step

(see section 3). If the mass loss causes no loss of diatom-bound N, as supported by the observation that N content increases upon treatment with hot deionized water (Table 2), then the amount of N removed by the oxidation is ≥8 μmol g^{-1} microfossils (Figures 3b and 4). Given the $\delta^{15}N$ difference between the cleaned diatoms and the bulk sediment the $\delta^{15}N$ of the N lost during oxidation is calculated to be as high as 13‰ (Figure 4).

The isotopic enrichment of the removed N raises the concern that the perchloric acid treatment somehow alters the isotopic composition of the sedimentary organic matter, rather than removing an isotopically distinct N pool. However, several points argue against this possibility. First, the use of other oxidants yields similar isotopic values. Although differences as great as 1‰ have been noted for different oxidants, the oxidized fraction is always significantly lighter than the unoxidized sediment, regardless of the oxidant used (Table 2). Second, the $\delta^{15}N$ depth profile for diatom-bound N has less structure than the profile of unoxidized sediment, so that diatom-bound $\delta^{15}N$ does not behave simply as bulk sediment $\delta^{15}N$ with an isotopic offset (Figure 3a). This same observation arises from the other components of our study as well. Third, the $\delta^{15}N$ of diatom ooze changes within the first hour of perchloric acid treatment but does not continue to change over longer periods of treatment (Figure 2a). If isotopic alteration of the entire sedimentary N pool was responsible for the $\delta^{15}N$ change, it would need to occur quickly and then cease altogether, which seems unlikely. Given these observations, the removal of an isotopically enriched N pool is the best explanation for the $\delta^{15}N$ change observed upon oxidative treatment.

If the isotopic enrichment of the vulnerable N pool was due to degradation with a constant isotope effect, then the $\delta^{15}N$ of the N removed by perchloric acid treatment would increase as the amount of N removed decreases according to Rayleigh fraction (Figure 4, dashed line) [*Marriotti et al.*, 1981]. However, the data do not appear to follow a Rayleigh fractionation trend. A better fit to the data is achieved if we assume that there are two distinct N pools with different $\delta^{15}N$ values, one of which is preferentially degraded (Figure 4, solid line). We would not argue that the fit to this latter model is good. Nevertheless, models with multiple N pools such as the two-pool model result in trends with more curvature in the space of Figure 4 than the Rayleigh fractionation trend, which is qualitatively what the data require. Thus the trend of the data leads us to favor a model of multiple discrete sedimentary N pools which degrade on different time scales (e.g., the "multi-G" model [*Berner*, 1980]) over a model of a single N pool which is progressively altered by fractionation during degradation.

4.2. Meridional Variations in Southern Ocean Sediments

Bulk sediment $\delta^{15}N$ increases to the north in the meridional transect of the ANTARES 1 multicores (Figure 5a). A similar increase in bulk sediment $\delta^{15}N$ observed in the east Indian sector has been interpreted as reflecting the meridional gradient in nitrate utilization [*Francois et al.*, 1992, 1997]. The bulk $\delta^{15}N$ gradient across the transect of cores used in this study is only 2-3‰ (Figure 5a). Surface sediments further to the north increase to 7.5‰ (not shown here), yielding a total northward increase of ~3.5‰ for bulk sediment $\delta^{15}N$. This change is lower than the 6-8‰ northward increase observed in the eastern Indian sector [*Francois et al.*, 1992, 1997] and is mostly associated with the $\delta^{15}N$ change into the high-opal Antarctic sediments south of 50°S.

Diatom-bound $\delta^{15}N$ shows a northward increase of 2.5-3‰ for sediment samples taken from 4-5 cm depth (Figure 5a). In order to compare this gradient with expectations we apply the Rayleigh fractionation model to the observed surface nitrate concentrations (Figure 5c). The southern end of the transect underlies Antarctic surface waters with nitrate concentrations of 25-27.5 μM, while the most northerly core in our study underlies the Polar Frontal Zone with surface water containing 18 μM nitrate (Figure 5c) [*Bianchi et al.*, 1997], although these concentrations, which were measured in April, may be higher than during the summertime production maximum. There are two Rayleigh fractionation equations for the particulate N generated from nitrate uptake, the instantaneous product equation and the integrated product equation [*Mariotti et al.*, 1981]. As described in section 5, the $\delta^{15}N$ of the sinking flux is expected to follow the instantaneous product equation when nitrate is consumed progressively during lateral transport, while it should follow the integrated product equation when surface nitrate concentrations reflect a more local balance of vertical nitrate supply and phytoplankton uptake [*Altabet and Francois*, 1994a, 1994b]. Assuming that the isotope effect of nitrate uptake is 5‰ (Sigman et al., submitted manuscript, 1998b) and using the nitrate concentrations collected during ANTARES 1, the expected meridional change in sinking flux $\delta^{15}N$ is 0.9‰ using the integrated product Rayleigh fractionation equation and 2.25‰ using the instantaneous product Rayleigh fractionation equation (Figure 5c and section 5). Thus the diatom $\delta^{15}N$ data appear to support the use of the instantaneous product equation across the Polar Frontal Zone, which applies in cases where nitrate supply is largely by net northward transport in the surface layer (see section 5). This matches the picture of nitrate transport which has arisen for the Subantarctic Zone, just to the north of the Polar Frontal Zone (Sigman et al., submitted manuscript, 1998b). On the other hand, if we learn in the future that the integrated product Rayleigh equation should apply in the Polar Frontal Zone, then the meridional $\delta^{15}N$ gradient observed in the uppermost sediments is greater than expected from the observed gradient in nitrate concentration. In this case we might infer that diatom-bound $\delta^{15}N$ is overly sensitive to nitrate utilization, varying more than we expect the $\delta^{15}N$ of the sinking flux to vary.

However, the significance of such comparisons is uncertain, because of a discrepancy between surface ocean conditions and sediment characteristics which was noted in the benthic studies of ANTARES 1 [*De Wit et al.*, 1997; *Riaux-Gobin et al.*, 1997; *Talbot and Bianchi*, 1997]. The Subantarctic Zone is greatly constricted at this longitude (Figure 1), leading to an unusually high velocity in the core of the Antarctic Circumpolar Current (ACC) [*Park and Gamberoni*, 1997]. Biological production appears to be highest at the sharp nutrient concentration gradient found at 43°-46°S [*Riaux-Gobin et al.*, 1997]. The intense barotropic flow of the ACC appears to transport the biogenic detritus away from the axis of greatest velocity at 45°-46°S, resulting in the redistribution of recent organic-rich material to the south, as suggested by the meridional distribu-

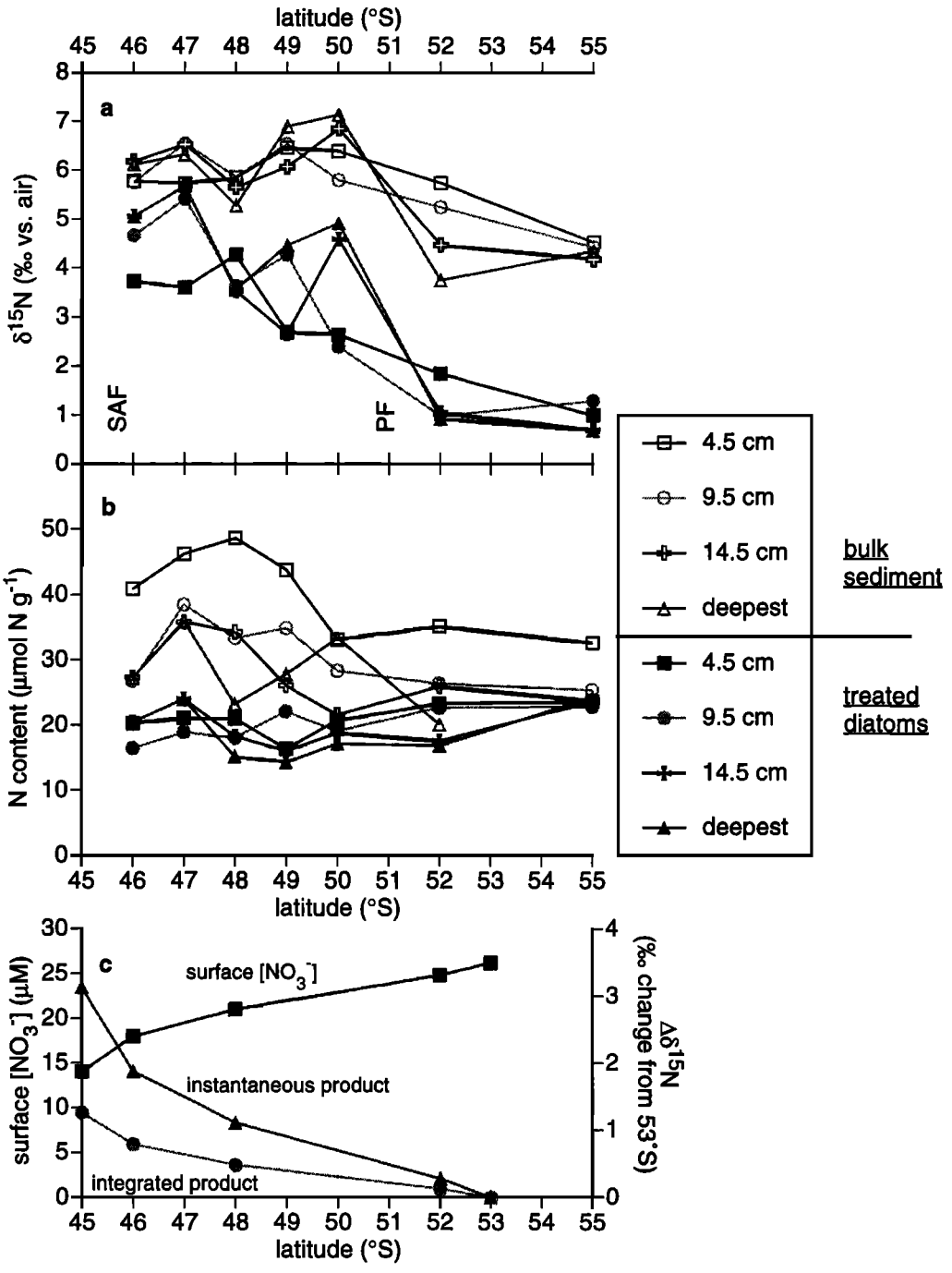

Figure 5. (a) $\delta^{15}N$ and (b) N content versus latitude for bulk sediment (open symbols) and the diatom-bound N fraction (solid symbols) at several depths in the meridional transect of multicores from ANTARES 1. Plotted values are the means of at least duplicate analyses. The approximate locations of the SAF and PF are shown [*Park and Gamberoni*, 1997]. (c) Surface nitrate (plus nitrite) concentrations (solid squares) were measured during ANTARES 1 in late austral Fall (April-May, 1993) [*Bianchi et al.*, 1997], and the expected northward increase in sinking flux $\delta^{15}N$ based on these nitrate concentrations and an isotope effect of 5‰ for nitrate uptake are calculated assuming the instantaneous product equation (solid triangles) and integrated product equation (solid circles) of Rayleigh fractionation (see Figures 9 and 10).

tions of sedimentary N (Figure 5b), sediment respiration rates [*De Wit et al.*, 1997], microphyte pigments [*Riaux-Gobin et al.*, 1997], and bacterial proteolytic activity [*Talbot and Bianchi*, 1997]. The occurrence of coastal benthic diatoms in the more northern cores also attests to the importance of lateral transport in this high energy environment [*Riaux-Gobin et al.*, 1997]. Since cumulative nitrate utilization increases to the north, meridional transport or exchange of biogenic detritus would deliver organic detritus and diatoms with a high $\delta^{15}N$ to our more northern cores, providing an alternative explanation

for the large diatom $\delta^{15}N$ gradient which we observe between 48°S and 55°S. Given the unknowns, the meridional gradient in surface sediments provides only qualitative confirmation of a link between nitrate utilization and diatom $\delta^{15}N$. Evaluation of the various potential factors in the observed meridional gradient of diatom-bound $\delta^{15}N$ will require complementary studies of isotope dynamics in the surface ocean, in sinking material, and in the sediments.

Downcore changes in both bulk sediment and diatom-bound $\delta^{15}N$ are evident in the ANTARES 1 multicores (Figure 5a). Below 5-10 cm depth in the more northern multicores, there are high values for both bulk and diatom-bound $\delta^{15}N$ which are inconsistent with the monotonic northward increase in nitrate utilization (Figure 5a). A depth profile of KTB 13 shows that diatom-bound $\delta^{15}N$ increases sharply below 12 cm (Figure 6a). At this same depth, aluminum content increases, indicating higher aluminosilicate concentrations in the deeper part of the core, while sedimentary barium decreases (Figure 6c). The $\delta^{15}N$, aluminum, and barium data are all consistent with the interpretation that KTB 13 represents a condensed stratigraphic section, with the last glacial/interglacial transition occurring at a depth of only ~14 cm [*Francois et al.*, 1997]. The occurrence of the glacial/interglacial transition at 14 cm would indicate a low Holocene sedimentation rate, <1 cm kyr^{-1}. While we do not have similar ancillary data for other cores, we suggest that this same stratigraphic transition also occurs in the cores to the north of KTB 13, explaining the downcore increases in diatom $\delta^{15}N$ observed in KTB 11, 19, and 21. Low sedimentation rate, winnowing, and scouring are common under the ACC, especially where the frontal structure is compressed [*Heezen and Hollister*, 1971], providing support for our inference of low sedimentation rates.

The diatom-bound N content is relatively uniform among the different cores, in contrast to the large meridional variation in bulk sediment N content (Figure 5 b). This corroborates the evidence from section 4.1 that diatom-bound N does not vary because of early diagenetic or sedimentary processes. If there is a meridional trend in the diatom-bound N content data, it is of higher N content in the more southern sediments, which are diatom oozes. In these sediments, diatom-bound N content is most similar to the N content of the bulk sediment, while the $\delta^{15}N$ differences between diatom-bound N and bulk sediment are greatest (up to 4‰, Figure 5a). This suggests that the $\delta^{15}N$ of the diagenetically vulnerable N increases as the size of this N pool decreases, as is also inferred from the results reported in section 4.1.

Diatom-bound N content appears to decrease with depth in cores KTB 6 (52°S) and KTB 13 (50°S), KTB 11 (49°S), and KTB 16 (48°S, Figures 5b and 6b). In the paleoceanographic profiles described in the following section, there is evidence for a similar gradual decrease in diatom-bound N content with age. This decrease is probably apparent in the ANTARES 1 multicores because of low sedimentation rates. Thus diatom-bound N may undergo gradual alteration on a time scale of ≥10 kyr. This is a concern for paleoceanographic work on longer time scales.

4.3. Paleoceanographic Records From the Antarctic

Both gravity core AII 107-22 from the Atlantic Antarctic and piston core MD 84-552 from the Indian Antarctic show the glacial/interglacial change in bulk sediment $\delta^{15}N$ which has been recognized throughout the Antarctic Zone (Figures 7 and 8) [*Francois et al.*, 1997]. The higher $\delta^{15}N$ values of the glacial age sediment have been interpreted as reflecting a higher degree of nitrate utilization in the Antarctic during the last ice age. However, the bulk $\delta^{15}N$ records differ substantially be-

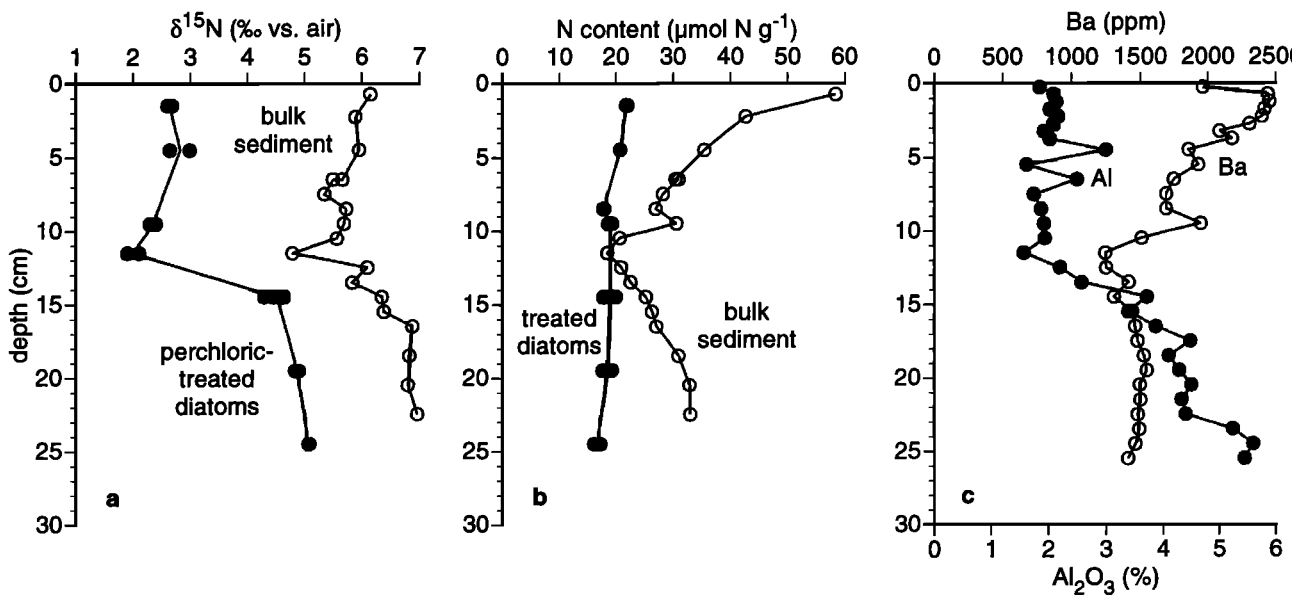

Figure 6. Depth profiles in core KTB 13 (50°S) of (a) $\delta^{15}N$ and (b) N content for both bulk N and diatom-bound N. Replicate analyses are shown, with solid lines connecting the mean values. (c) Depth profiles of sedimentary Ba and Al content are shown to demonstrate a stratigraphic change at ~12 cm depth. These data suggest that glacial-age sediments occur at 15 cm, which implies average Holocene sedimentation rates of <1 cm yr^{-1}.

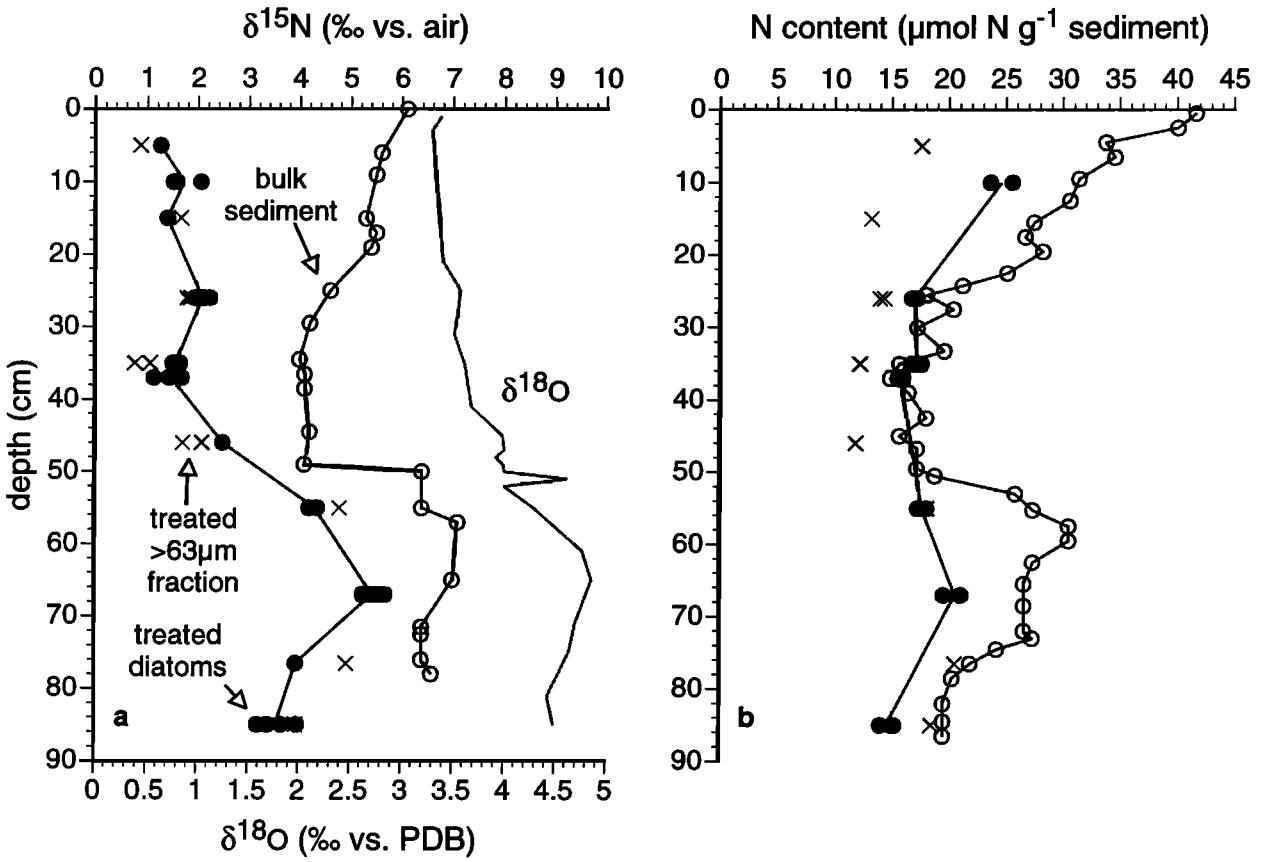

Figure 7. Depth profiles in gravity core AII 107-22 (Antarctic Zone, Atlantic Sector, 55°S, 3°W, 2768 m) of (a) $\delta^{15}N$ and (b) N content of bulk N (open circles), diatom N (solid circles), and the perchloric acid-treated >63 μm fraction (crosses), which is composed of large diatoms, radiolaria, and some detrital grains. Replicate analyses are shown for the cleaned diatom and >63 μm fractions, with solid lines connecting the mean values for the diatom N analyses. The N content of the bulk sediment is in some cases lower than that of the diatom fraction because of the presence of dense detrital grains in the bulk sediment. The planktonic foraminiferal $\delta^{18}O$ stratigraphy [from *Keigwin and Boyle*, 1989] suggests that sediment from the Last Glacial Maximum is at 65 cm depth.

tween these cores. In AII 107-22, the maximum glacial/interglacial difference in bulk $\delta^{15}N$ is the ~2‰ shift at 50 cm, but bulk $\delta^{15}N$ increases back to higher values near the top of the core. In MD 84-552 the glacial sediments are up to 5‰ higher in $\delta^{15}N$ than the Holocene sediments, and the Holocene section does not show a significant increase toward the top of the core. If these changes are interpreted strictly in terms of nitrate utilization, they imply very different histories of nitrate utilization for these two sectors of the Antarctic since the last ice age. For instance, the bulk sediment $\delta^{15}N$ increase within the Holocene section of AII 107-22 would imply that nitrate utilization in the Atlantic sector has increased over the course of the Holocene back to near-glacial levels.

The diatom-bound $\delta^{15}N$ records show the same sense of glacial/interglacial change as the bulk sediment $\delta^{15}N$ records, with higher values in the glacial section (Figures 7 and 8). This indicates that the fundamental glacial/interglacial bulk sediment $\delta^{15}N$ change observed in the Antarctic was not due to diagenetic processes, suggesting that the $\delta^{15}N$ of the N sinking flux in the Antarctic was indeed higher during the last ice age.

While the amplitude of the glacial/interglacial change differs significantly for the two bulk sediment records, the diatom $\delta^{15}N$ records are more similar to one another. Although the depth resolution of the diatom $\delta^{15}N$ samples is too sparse to allow for a rigorous comparison, the glacial/interglacial amplitude for both cores is ~4‰. On the basis of these diatom $\delta^{15}N$ data we conclude that the glacial/interglacial change in the $\delta^{15}N$ of the sinking flux was similar in the Atlantic and Indian sectors of the Southern Ocean, as might be expected given the continuity of zonal circulation in these sectors of the Southern Ocean. The greater consistency between the two diatom $\delta^{15}N$ records may indicate that they provide a more reliable record of sinking flux changes than do the bulk sediment records. For instance, in light of the diatom $\delta^{15}N$ record from AII 107-22, the bulk sediment $\delta^{15}N$ change in the top 30 cm of AII 107-22 could be interpreted as an early diagenetic change associated with the loss of diagenetically vulnerable sedimentary N during burial (Figure 7).

5. Discussion: Glacial/Interglacial Changes in the Antarctic

Our diatom N results support the conclusion, reached previously from bulk sediment $\delta^{15}N$ data, that the sinking flux $\delta^{15}N$ in the Antarctic was higher during the last ice age [*Francois et*

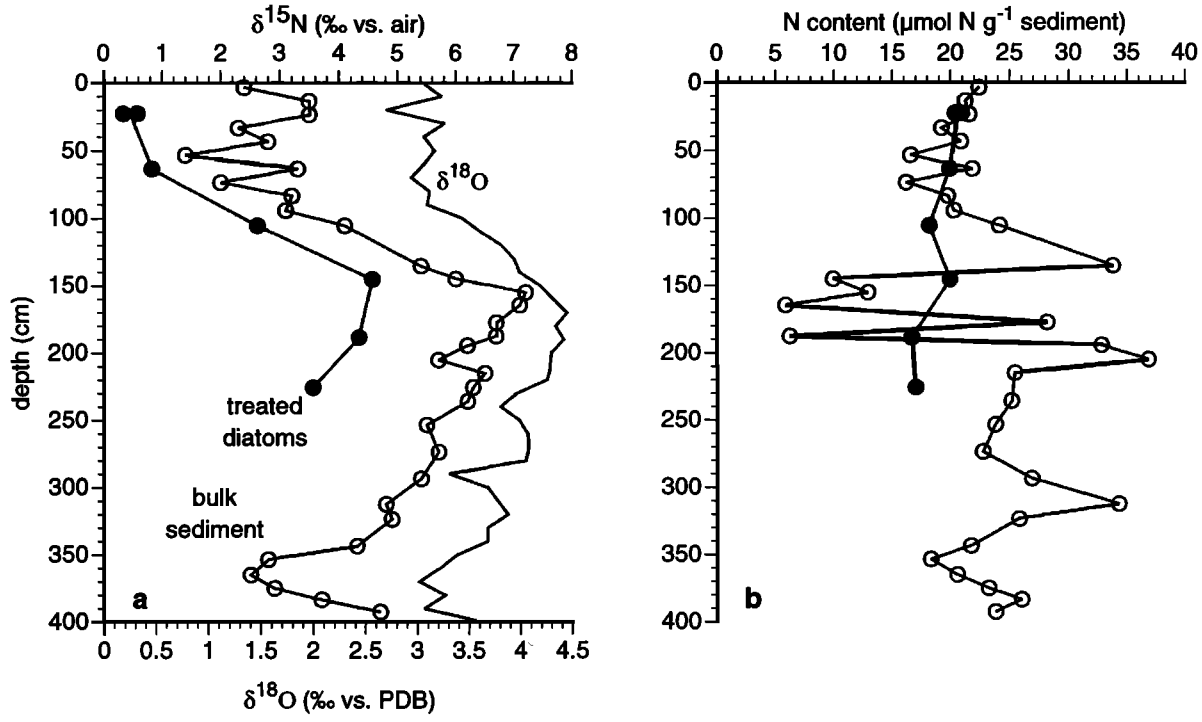

Figure 8. Depth profiles in piston core MD 84-552 (Antarctic Zone, Indian Sector, 55°S, 74°E, 2230 m) of (a) $\delta^{15}N$ and (b) N content of bulk sediment N (open circles) and diatom-bound N (solid circles). Replicate analyses are shown for the treated diatom fraction, with solid lines connecting the mean values. The planktonic foraminiferal $\delta^{18}O$ stratigraphy shown in Figure 8a suggests that sediment from the Last Glacial Maximum is at 170 cm depth (L.D. Labeyrie, personal communication, 1996). As in AII 107-22, the N content of the bulk sediment is lowered by the presence of detrital grains, especially in the glacial section.

al., 1992, 1997]. Given the role of nitrate utilization in the N isotope dynamics of the modern Antarctic, it is reasonable to interpret this change in sinking flux $\delta^{15}N$ in terms of nitrate utilization. The nitrate utilization/N isotope relationship in the modern Antarctic approximates the Rayleigh fractionation model in which the surface layer nitrate pool is progressively consumed by phytoplankton over the course of the summer season, with nitrate uptake having an isotope effect of 5±1‰ (Figure 9a) (Sigman et al., submitted manuscript, 1998b). Upper Circumpolar Deep Water, the ultimate source of nitrate to the modern Antarctic surface, has a $\delta^{15}N$ of ~5‰ (Sigman et al., submitted manuscript, 1998a). If it is assumed that these parameters have not changed dramatically over the last glacial/interglacial cycle, then the ~4‰ shift in the sinking flux $\delta^{15}N$ inferred from the diatom N data suggests that the degree of nitrate utilization was higher in the glacial Antarctic.

Quantifying the inferred utilization change from the $\delta^{15}N$ data requires further assumptions. The integrated product equation of Rayleigh fractionation would describe the $\delta^{15}N$ of the sinking flux out of the surface ocean if the nitrate supply to the Antarctic surface is dominated by vertical mixing during the winter (Figures 9a and 10a) [*Altabet and Francois*, 1994a, 1994b]. On the other hand, if equatorward advection of a progressively consumed surface nitrate pool dominates the nitrate supply, then the relationship between the degree of nitrate utilization and the $\delta^{15}N$ of the sinking flux would more closely approximate the instantaneous product equation (Figures 9a and 10b). These two possibilities cannot be distinguished using Antarctic nitrate $\delta^{15}N$ data (Figure 10), requiring the use of other constraints.

The advective circulation of the Antarctic is composed of Ekman-driven net equatorward flow of surface water fed by the diffuse upwelling of Circumpolar Deep Water [*Gordon et al.*, 1977]. This advective circulation leads to both vertical and lateral fluxes of nitrate (Figure 10c). Combining this circulation with the seasonal vertical mixing known to occur in the Antarctic [*Gordon and Huber*, 1990; *Martinson*, 1990], there should be components of both vertical and lateral nitrate supply within the Antarctic, and we would expect the sinking flux out of the Antarctic to follow a $\delta^{15}N$/nitrate utilization relationship which is intermediate between the integrated product and instantaneous product equations.

The uniformity of surface nitrate concentration reflects the importance of lateral and vertical mixing in the modern Antarctic. It suggests that the $\delta^{15}N$ of the sinking flux should be relatively constant across the Antarctic and should approximate the integrated product Rayleigh equation. This view is supported by the bulk sediment $\delta^{15}N$ data [*Francois et al.*, 1997] and the available sediment trap $\delta^{15}N$ data (M. Altabet and R. Francois, unpublished results, 1998). However, lateral nitrate transport and progressive utilization may have dominated during the last ice age because of more complete nitrate consumption (by analogy with the modern Subantarctic (Sigman et al., submitted manuscript, 1998b)), in which case the instantaneous product Rayleigh equation would have been more appropriate for the glacial Antarctic. If we assume that the integrated product equation applies in the modern Antarctic, then a 4‰ $\delta^{15}N$ increase in the sinking flux suggests a 35-75% increase in nitrate utilization, that is, 60-100% utilization in the glacial Antarctic compared to 25% in the modern Antarctic (Figure

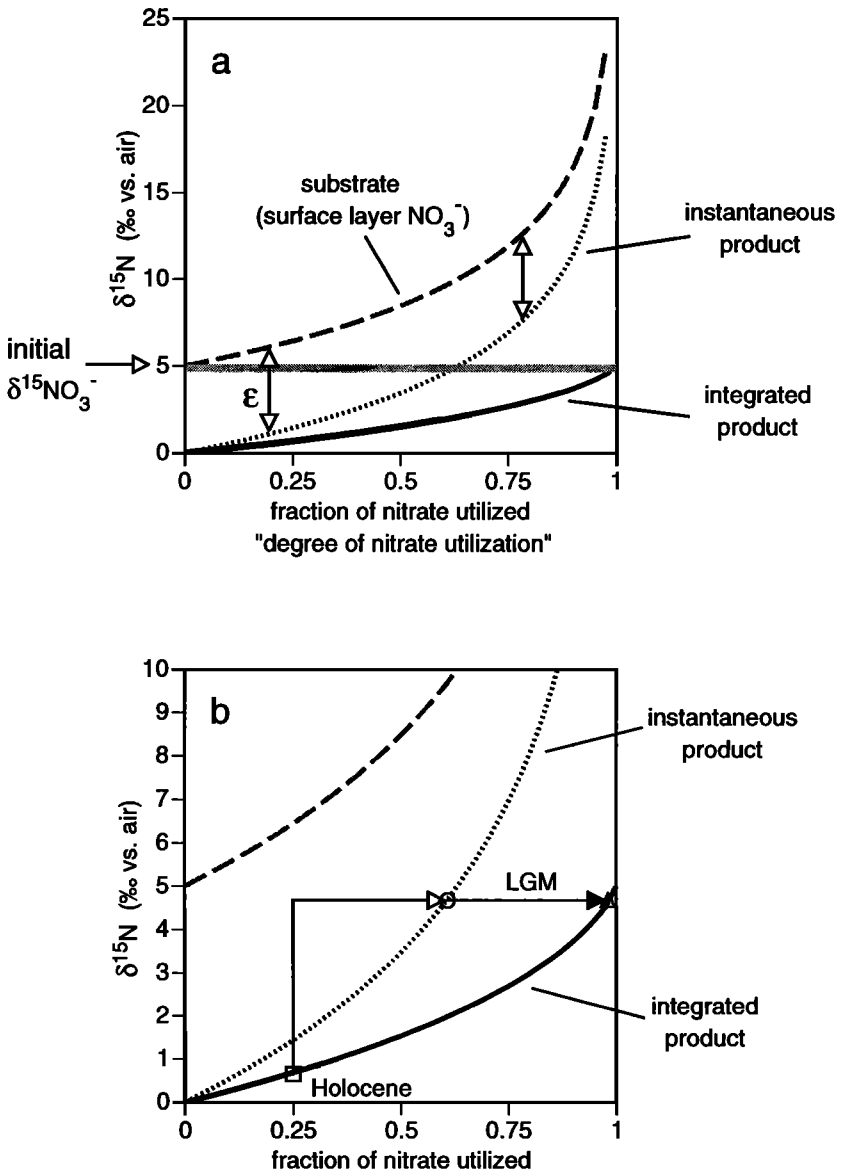

Figure 9. (a) A plot of the Rayleigh fractionation equations shows the theoretical link between nitrate utilization and the $\delta^{15}N$ of the different N pools. The instantaneous product equation describes the $\delta^{15}N$ of N being extracted from the surface layer nitrate pool at a given degree of nitrate utilization. The integrated product equation describes the $\delta^{15}N$ of the entire N pool that has been drawn from the nitrate pool to achieve a given degree of nitrate utilization. The $\delta^{15}N$ of the initial nitrate supply and the isotope effect of nitrate uptake (ε) are both set at 5‰, as is appropriate for the modern Antarctic [*Sigman*, 1997]. (b) A blow-up of Figure 9a to illustrate the range of glacial/interglacial changes in nitrate utilization inferred from a 4‰ change in the $\delta^{15}N$ of the sinking flux. If the integrated product equation was appropriate for the glacial Antarctic (solid arrow), then the inferred utilization of the Last Glacial Maximum (LGM) was nearly complete (open triangle). If the instantaneous product equation is appropriate (open arrow), then the inferred utilization during the last glacial was 60% (open circle). In both cases, Holocene Antarctic nitrate utilization is set at 25%, and the integrated product equation is assumed to apply during the Holocene (open square).

9b). The extremes of this range correspond to the end-member assumptions of the instantaneous product equation and the integrated product equation for the glacial Antarctic. Using these two end-members to define the range of possibilities, Antarctic nitrate utilization was 60% or greater during the last ice age, given the above assumptions.

We should note that a continuous steady state between nitrate uptake by phytoplankton and nitrate supply from below, as opposed to the Rayleigh model of wintertime nitrate supply and summertime nitrate uptake, yields a relationship between nitrate utilization and $\delta^{15}N$ which is similar to that of the integrated product equation of Rayleigh fractionation. Thus, estimates of the apparent utilization change based on this model would be similar to those based on the integrated product equation of Rayleigh fractionation. We do not discuss the continuous supply model further because a steady state balance be-

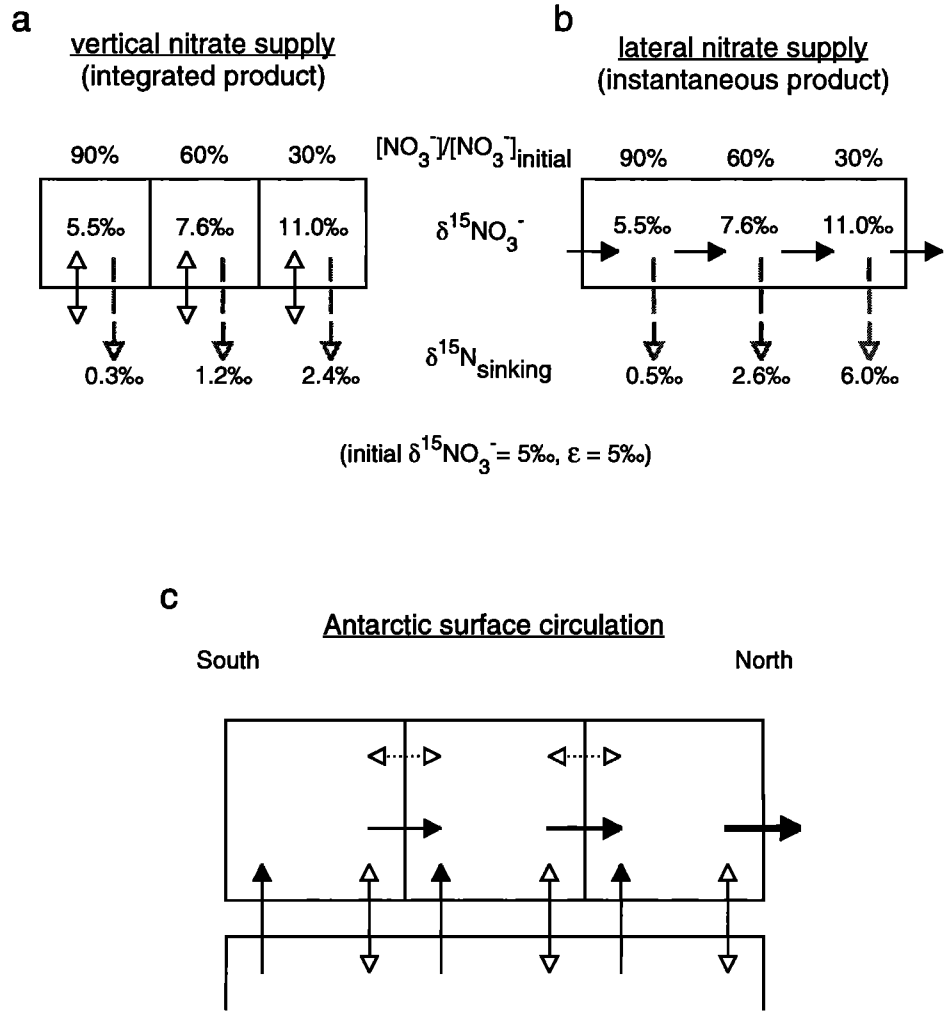

Figure 10. (a) and (b) Cartoons of the relationship between nitrate utilization and the $\delta^{15}N$ of the sinking flux. If nitrate is supplied vertically every winter (Figure 10a), then utilization during the summer occurs in nitrate with an initial $\delta^{15}N$ of 5‰. In this case, the $\delta^{15}N$ of the sinking flux out of any surface box over the course of the year is described by the integrated product Rayleigh equation. If instead nitrate is supplied laterally from other surface regions (Figure 10b), then the $\delta^{15}N$ of the nitrate supply to the downstream sites is ≥5‰. In a surface layer with a lateral gradient in nitrate concentration due to progressive nitrate utilization and unidirectional water transport (and assuming no lateral organic N transport) the $\delta^{15}N$ of the sinking flux follows the instantaneous product Rayleigh equation (c) In the Antarctic, there are both advective and vertical fluxes of nitrate. Seasonal mixing (open arrows) supplies nitrate from Circumpolar Deep Water. Ekman divergence (solid arrows) results in components of both vertical and lateral nitrate supply. Lateral mixing (open arrows and dashed lines) works to homogenize the Antarctic surface, erasing any pattern of progressive utilization across the Antarctic. Observations suggest that the vertical transport and mixing terms dominate, so that the sinking flux out of the modern Antarctic should follow the integrated product equation. However, the situation may have been different during the last glacial period.

tween nitrate supply and uptake is not supported by observations from the Antarctic (Sigman et al., submitted manuscripts, 1998a, 1998b).

An alternative explanation for the observed glacial/interglacial $\delta^{15}N$ change is that some aspect of the fractionation process has changed on glacial/interglacial time scales. The two key parameters in this regard are (1) the isotope effect of nitrate uptake and (2) the $\delta^{15}N$ of the initial nitrate supply (Figure 9a).

Taking the different culture-based estimates at face value, there is potential for large variations in the isotope effect of nitrate uptake [*Wada and Hattori*, 1978; *Wada*, 1980; *Montoya and McCarthy*, 1995; *Pennock et al.*, 1996; *Waser et al.*, 1998]. However, the most recent studies report a relatively narrow range of variation in the isotope effect (e.g., 4.5-6.3‰ for the diatom *Thalassiosira pseudonana* [*Waser et al.*, 1998]). The field-based estimates of the isotope effect are remarkably similar relative to our ability to estimate it (5±1‰ over a range of modern environments [*Sigman*, 1997; *Wu et al.*, 1997; *Altabet et al.*, 1999]). While it remains possible that changes in the isotope effect have contributed to the glacial/interglacial $\delta^{15}N$ change of the Antarctic sinking flux, Antarctic $\delta^{15}NO_3$ results to date do not provide support for a ~4‰ lower isotope effect in the glacial Antarctic (Sigman et al., submitted manuscript, 1998b).

The $\delta^{15}N$ of the nitrate supply to the modern surface Antarctic is set by Circumpolar Deep Water, its ultimate nitrate source. In turn the nitrate $\delta^{15}N$ of Circumpolar Deep Water is

tied to the global deep water value of ~5‰ (Sigman et al., submitted manuscript, 1998a). Assuming the same deep ocean isotopic homogeneity during the last glacial period, the $\delta^{15}N$ of the nitrate supply to the Antarctic would have reflected the global deep nitrate $\delta^{15}N$ of the glacial ocean. Therefore, we must ask whether the $\delta^{15}N$ of nitrate in glacial deep water may have been higher.

Attempts to test for a glacial/interglacial change in the $\delta^{15}N$ of oceanic nitrate have focused on downcore records from subtropical regions, where nitrate is being supplied to the surface from the thermocline and intermediate depth ocean (J. Farrell and T. Pederson, unpublished results, 1997; M. Altabet, unpublished results, 1998). Published data show no discernible glacial/interglacial change in these environments [*Francois et al.*, 1997]. This argues against a large change in the mean $\delta^{15}N$ of thermocline nitrate over glacial/interglacial cycles.

In ocean geochemistry models, enhanced polar nutrient utilization drives a decrease in the mean oxygen concentration of the ocean interior [*Knox and McElroy*, 1984; *Sarmiento and Toggweiler*, 1984; *Siegenthaler and Wenk*, 1984]. This oxygen decrease occurs mostly in the deep ocean, below thermocline and intermediate depth waters (Figure 11) [*Keir*, 1988, 1990; *Sarmiento and Orr*, 1991]. The redistribution of nutrients and oxygen between the intermediate and deep ocean, first proposed by *Boyle* [1988] as "nutrient deepening," is supported by evidence of nutrient depletion and higher oxygen concentrations at intermediate depths [e.g., *Boyle and Keigwin*, 1982; *Oppo and Fairbanks*, 1987; *Kallel et al.*, 1988; *Herguera et al.*, 1992; *Boyle et al.*, 1995; *Kennet and Ingram*, 1995] and lower oxygen concentrations in the deep ocean [*Francois et al.*, 1997].

In the intermediate depth low-oxygen zones of the modern ocean, denitrification causes isotopic enrichment of nitrate [*Cline and Kaplan*, 1975; *Liu and Kaplan*, 1989; *Brandes et al.*, 1998]. During the last glacial, higher oxygen concentrations at intermediate depths apparently suppressed denitrification at these depths [*Altabet et al.*, 1995; *Ganeshram et al.*, 1995]. If low-oxygen zones shifted into the deeper ocean during the last ice age, then denitrification might have become a deep ocean phenomenon, leading to zones of high nitrate $\delta^{15}N$ in the deep ocean. Since Circumpolar Deep Water exchanges directly with the abyssal waters of the global ocean, any such increase in the $\delta^{15}N$ of deep ocean nitrate would have increased the $\delta^{15}N$ of the nitrate supply to the Antarctic surface.

The isotopic signal of denitrification in the modern intermediate depth ocean diminishes rapidly away from the regions of denitrification. For instance, thermocline $\delta^{15}NO_3$ decreases from ≥15‰ near the eastern margin of the tropical Pacific to ≤6‰ on the same isopycnal near Hawaii, only ~1‰ higher than the apparent mean value for deep ocean nitrate $\delta^{15}N$ [*Cline*

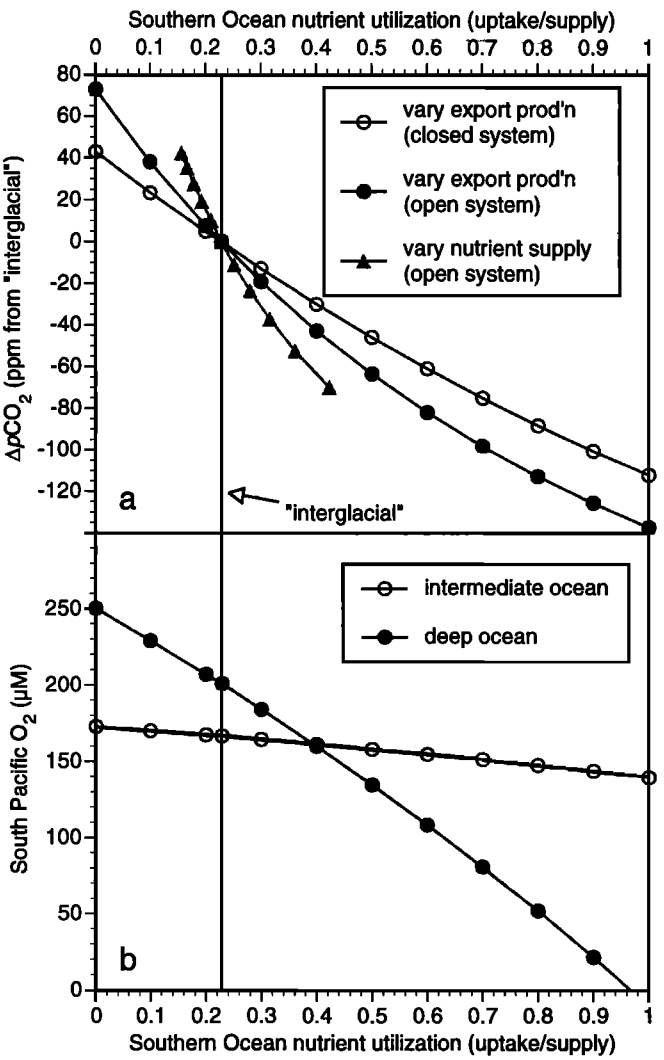

Figure 11. The response of (a) atmospheric CO_2 and (b) subsurface O_2 to changes in Southern Ocean nutrient utilization in the Cyclops model [*Keir*, 1988]. In the interglacial standard case, nutrient utilization is 23% (vertical line). That is, 23% of the gross nitrate and phosphate supply to the Southern Ocean surface is consumed by phytoplankton before the surface water descends back into the subsurface as newly formed intermediate water or deep water (for the circulation, see *Keir* [1988] or *Sigman et al.* [1998]). In one set of experiments, nutrient utilization is altered by varying export production (circles in both Figure 11a and Figure 11b). The atmospheric CO_2 response is calculated with and without the effect of the oceanic $CaCO_3$ balance (solid and open circles, respectively) [*Sigman et al.*, 1998]. The greater CO_2 response of the open system case (which includes the oceanic $CaCO_3$ balance) is largely due to a transient dissolution event which occurs in the deep sea in response to a utilization increase [*Broecker and Peng*, 1987]. As pointed out by *Keir* [1988, 1990] and *Sarmiento and Orr* [1991], the O_2 decrease in the subsurface is focused in the deep sea (solid circles in Figure 11b), with intermediate depth and thermocline O_2 levels changing little (open circles). In a second set of experiments, utilization is varied by changing the vertical mixing rate in the Southern Ocean while maintaining a constant rate of export production in that region (solid triangles in Figure 11a). This experiment is more representative of the apparent glacial/interglacial changes in the Antarctic, with enhanced nitrate utilization during the last glacial period resulting from reduced nitrate supply rather than increased export production [*Francois et al.*, 1997]. When the vertical mixing rate is lowered, an increase to 42% nutrient utilization lowers atmospheric CO_2 by 70 ppm, compared to a 45 ppm decrease if utilization was increased to this level by enhanced export production. The cause for these different responses of atmospheric CO_2 to a given change in nitrate utilization will be described elsewhere. Any further increase in nutrient utilization due to reduced nutrient supply would require a more involved model experiment which includes changes in global ocean circulation. As vertical mixing is reduced in the Southern Ocean, steps are taken to prevent warming in the model deep ocean (a side effect of this experiment), since the deep ocean was colder during the last glacial period [*Schrag and DePaolo*, 1993].

and Kaplan, 1975; Sigman et al., submitted manuscript, 1998a; M. Altabet, unpublished results, 1998]. If denitrification occurred in the deep ocean during the last glacial period, its isotopic signal would have been diluted over the large volume of abyssal waters. Given the evidence against a large change in the $\delta^{15}N$ of the thermocline nitrate, it seems unlikely that a deep ocean denitrification signal could have caused more than a 1‰ increase in the $\delta^{15}N$ of deep nitrate during the last glacial period, so that it could explain only a portion of the observed glacial/interglacial change in Antarctic diatom $\delta^{15}N$. Moreover, a decrease in deep ocean oxygen requires a cause, and the inferred increase in polar nutrient utilization is a particularly suitable candidate [*Keir*, 1988, 1990].

Despite these and other uncertainties in the translation of diatom $\delta^{15}N$ to nitrate utilization it is worth considering the potential effect of the inferred utilization changes on atmospheric CO_2. Using the "Cyclops" ocean geochemistry model [*Keir*, 1988; *Sigman et al.*, 1998] to provide an estimate of the expected carbon cycle response to enhanced nitrate utilization, we find that 25-40% higher nitrate utilization (i.e., 50-65% in the glacial ocean compared to 25% during the present interglacial) would lower atmospheric CO_2 by ~80 ppm (Figure 11), which is comparable to the glacial/interglacial atmospheric CO_2 variations observed in ice core records [*Barnola et al.*, 1987]. This calculation must be considered in the context of the uncertainties described above. Even if the interpreted change in Antarctic nitrate utilization is correct, the Subantarctic remains poorly understood with regard to nutrient supply and uptake during the last ice age, and this region is also represented by the Southern Ocean surface box in the Cyclops model. Nevertheless, our results provide motivation for a renewed consideration of the Southern Ocean as a driver of glacial/interglacial changes in atmospheric CO_2.

6. Conclusions

Unlike bulk sedimentary N, diatom-bound N does not appear to be isotopically altered by early bacterial diagenesis, making it a useful tool for paleoceanographic studies. Our data suggest that it survives early diagenesis because of physical protection within the opal matrix. Chemical composition and fluorescence microscopy data to be presented elsewhere corroborate this interpretation, suggesting that the diatom-bound N is native to the diatoms [*Sigman*, 1997]. The $\delta^{15}N$ of diatom-bound N, like that of the integrated sinking flux and bulk sediment, appears to vary with the degree of nitrate utilization in Southern Ocean surface waters, although the quantitative nature of the link has not been fully demonstrated. In any case, given the evidence for a Rayleigh fractionation-like process associated with nitrate uptake in Southern Ocean surface waters (Sigman et al., submitted manuscript, 1998b) and the recognized importance of diatoms in nitrate uptake [*Dugdale and Wilkerson*, 1998], this relationship is to be expected.

Our downcore results on diatom-bound N suggest that the $\delta^{15}N$ of the sinking flux was 3-4‰ higher during the last glacial period, supporting the interpretation that the previously reported glacial/interglacial change in bulk sediment $\delta^{15}N$ had its origins in the upper ocean, rather than being due to diagenetic or sedimentary processes. Given our understanding of Southern Ocean N isotope dynamics, a change in nitrate utilization in Antarctic surface waters is the simplest explanation for the glacial/interglacial change in the $\delta^{15}N$ of the sinking flux. While there are many uncertainties, we estimate that the diatom $\delta^{15}N$ change would correspond to an increase in utilization of 40% or more, making it a potential explanation for observed glacial/interglacial atmospheric CO_2 changes.

Paleoceanographic proxy data demonstrate that biogenic fluxes were reduced in the Antarctic Zone during the last ice age, suggesting that more complete nitrate utilization in the Antarctic was due to a lower rate of nitrate supply from the subsurface [*Francois et al.*, 1997], rather than an increase in export production. The cause for this change in the rate of nitrate supply remains an open question. A stronger Antarctic halocline [*Morley and Hays*, 1983], perhaps due to a more vigorous sea ice cycle [*Crosta et al.*, 1998], may have decreased the rates of vertical mixing and nitrate supply in the Antarctic. Alternatively, a northward shift in the wind field may have decreased the nitrate supply to the Antarctic through a reduction in Ekman divergence [*Toggweiler and Samuels*, 1995]. It is worth noting the consistency between the possibility of less Ekman divergence in the glacial Antarctic and the evidence for a glacial reduction in the formation rate of North Atlantic Deep Water [e.g., *Boyle and Keigwin*, 1982], which currently feeds the overturning circulation of the Southern Ocean.

Acknowledgments. J. Adkins, L. Eglinton, A. Shemesh, and J. Whelan provided valuable advice. The comments of E. Boyle motivated the discussion of deep ocean oxygen. Reviews by W. Broecker and two anonymous reviewers helped to improve the manuscript. The first author was supported by the NSF Graduate Research Fellowship Program and the JOI/USSAC Ocean Drilling Graduate Research Fellowship Program. This is WHOI contribution 9854.

References

Altabet, M.A. and R. Francois, Sedimentary nitrogen isotopic ratio as a recorder for surface ocean nitrate utilization. *Global Biogeochem. Cycles, 8*, 103-116, 1994a.

Altabet, M.A. and R. Francois, The use of nitrogen isotopic ratio for reconstruction of past changes in surface ocean nutrient utilization, *Carbon Cycling in the Glacial Ocean: Constraints on the Ocean's Role in Global Change*, edited by R. Zahn et al., NATO ASI Series, vol. 17, Springer-Verlag, New York, pp. 281-306, 1994b.

Altabet, M.A. and J.J. McCarthy, Temporal and spatial variation in the natural abundance of ^{15}N in PON from a warm-core ring, *Deep Sea Res., 32*, 755-772, 1985.

Altabet, M.A., W G. Deuser, S. Honjo, C. and Stienen, Seasonal and depth-related changes in the source of sinking particles in the North Atlantic, *Nature, 354*, 136-139, 1991.

Altabet, M.A., R. Francois, D.W. Murray, and W.L. Prell, Climate-related variations in denitrification in the Arabian Sea from sediment $^{15}N/^{14}N$ ratios, *Nature, 373*, 506-509, 1995.

Altabet, M.A., C. Pilskaln, R Thunell, C. Pride, D. Sigman, F. Chavez, and R. Francois, The Nitrogen isotope biogeochemistry of sinking particles from the margin of the eastern North Pacific, *Deep Sea Res. Part I*, in press, 1999.

Barnola, J.M., D. Raynaud, Y.S. Korotkevitch, and C. Lorius, Vostok ice core provides 160,000-year record of atmospheric CO_2, *Nature, 329*, 408-414, 1987.

Berner, R.A., *Early Diagenesis: A Theoretical Approach*, 241 pp., Princeton Univ. Press, Princeton, N.J., 1980.

Bianchi, M., F. Feliatra, P. Treguer, M.-A. Vincendeau, and J. Morvan, Nitrification rates, ammonium and nitrate distribution in upper layers of the water column and in sediments of the Indian sector of the Southern Ocean, *Deep Sea Res. Part II, 44*, 1017-1032, 1997.

Boyle, E.A.. The role of vertical chemical fractionation in controlling late quaternary atmospheric carbon dioxide, *J. Geophys. Res., 93*, 15,701-15,714, 1988.

Boyle, E.A , and L.D. Keigwin, Deep circulation of

the North Atlantic for the last 200,000 years: Geochemical evidence, *Science, 218*, 784-787, 1982.

Boyle, E.A., L. Labeyrie, and J.-C. Duplessy, Calcitic foraminiferal data confirmed by cadmium in aragonitic Hoeglundina: Application to the last glacial maximum in the northern Indian Ocean, *Paleoceanography, 10*, 881-900, 1995

Brandes, J.A., A.H. Devol, T. Yoshinari, D.A. Jayakumar, and S.W.A. Naqvi, Isotopic composition of nitrate in the central Arabian Sea and eastern tropical North Pacific: A tracer for mixing and nitrogen cycles, *Limnol. Oceanogr., 43*, 1680-1689, 1998.

Broecker, W.S., and T.-H. Peng, The role of $CaCO_3$ compensation in the glacial to interglacial atmospheric CO_2 change, *Global Biogeochemical Cycles, 1*, 15-29, 1987.

Broecker, W.S., and T.-H. Peng, The cause of the glacial to interglacial atmospheric CO_2 change: A polar alkalinity hypothesis, *Global Biogeochem. Cycles, 3*, 215-239.

Cline, J.D. and I.R. Kaplan, Isotopic fractionation of dissolved nitrate during denitrification in the eastern tropical North Pacific Ocean, *Mar. Chem., 3*, 271-299, 1975.

Crosta, X., J.-J. Pichon, and L.H. Burckle, Application of modern analogue technique to marine Antarctic diatoms: Reconstruction of maximum sea-ice extent at the Last Glacial Maximum, *Paleoceanography, 13*, 284-297, 1998.

De Wit, R., J.-C. Relexans, T. Bouvier, and D.J.W. Moriarty, Microbial respiration and diffusive oxygen uptake of deep-sea sediments in the Southern Ocean (ANTARES I cruise), *Deep Sea Res Part II, 44*, 1053-1068, 1997.

Dugdale, R.C. and F.P. Wilkerson, Silicate regulation of new production in the equatorial Pacific upwelling, *Nature, 391*, 270-273, 1998.

Farrell, J.W., T.F. Pedersen, S.E. Calvert, and B. Nielsen, Glacial-interglacial changes in nutrient utilization in the equatorial Pacific Ocean, *Nature, 377*, 514-517, 1995.

Francois, R., M.A. Altabet, and L.H. Burkle, Glacial to interglacial changes in surface nitrate utilization in the Indian sector of the Southern Ocean as recorded by sediment $\delta^{15}N$, *Paleoceanography, 7*, 589-606, 1992.

Francois, R., M.P. Bacon, M.A. Altabet, and L.D. Labeyrie, Glacial/intergalcial changes in sediment rain rate in the S.W. Indian sector of Subantarctic waters as recorded by ^{230}Th, ^{231}Pa, U, and $\delta^{15}N$, *Paleoceanography, 8*, 611-630, 1993.

Francois, R.F., M.A. Altabet, E.-F. Yu, D.M. Sigman, M.P. Bacon, M. Frank, G. Bohrmann, G. Bareille, and L.D. Labeyrie, Water column stratification in the Southern Ocean contributed to the lowering of glacial atmospheric CO_2, *Nature, 389*, 929-935, 1997.

Gaillard, J.-F., ANTARES-1: A biogeochemical study of the Indian sector of the Southern Ocean, *Deep Sea Res. Part II, 44*, 951-962, 1997.

Ganeshram, R.S., T.F. Pedersen, S.E. Calvert, and J.W. Murray, Large changes in oceanic nutrient inventories from glacial to interglacial periods, *Nature, 376*, 755-758, 1995.

Gordon, A.L., and B.A. Huber, Southern Ocean winter mixed layer, *J. Geophys. Res., 95*, 11655-11672, 1990.

Gordon, A.L., H.W. Taylor, and D.T. Georgi, Antarctic oceanographic zonation, in *Polar Oceans*, edited by M.J. Dunbar, Arct. Inst. of North Am., Calgary, Alberta, Can., 1977.

Hayes, J.M., B.N. Popp, R. Takigiku, and M.W. Johnson, An isotopic study of biogeochemical relationships between carbonates and organic carbon in the Greenhorn Formation, *Geochim. Cosmochim. Acta, 53*, 2961-2972, 1989.

Heezen, B.C. and C.D. Hollister, *The Face of the Deep*, 657 pp., Oxford Univ. Press, New York, 1971.

Herguera, J.C., E. Jansen, and W.H. Berger, Evidence for a bathyal front at 2000 m depth in the glacial Pacific, based on a depth transect on Ontong Java Plateau, *Paleoceanography, 7*, 273-288, 1992.

Jasper, J.P. and J.M. Hayes, A carbon-isotopic record of CO_2 levels during the late Quaternary, *Nature, 347*, 462-464, 1990.

Kallel, N., L.D. Labeyrie, A. Juillet-Leclerc, and J.-C. Duplessy, A deep hydrological front between intermediate and deep-water masses in the glacial Indian Ocean, *Nature, 333*, 651-655, 1988.

Keigwin, L.D. and E.A. Boyle, Late quaternary paleochemistry of high-latitude surface waters, *Paleogeogr. Palaeoclimatol. Paleoecol., 73*, 85-106, 1989

Keir, R.S., On the late Pleistocene ocean geochemistry and circulation, *Paleoceanography, 3*, 413-445, 1988.

Keir, R.S., Reconstructing the ocean carbon system variation during the last 150,000 years according to the Antarctic nutrient hypothesis, *Paleoceanography, 5*, 253-276, 1990.

Kennett, J.P. and B.L. Ingram, A 20,000-year record of ocean circulation and climate change from the Santa Barbara basin, *Nature, 377*, 510-514, 1995.

Knox, F. and M. McElroy, Changes in atmospheric CO_2 influence of the marine biota at high latitude, *J. Geophys. Res., 89*, 4629-4637, 1984.

Liu, K.-K. and I.R. Kaplan, The eastern tropical Pacific as a source of ^{15}N-enriched nitrate in seawater off southern California, *Limnol. Oceanogr., 34*, 820-830, 1989.

Macko, S.A., M.H. Engel, and P.L. Parker, Early diagenesis of organic matter in sediments: assessment of mechanisms and preservation by the use of isotopic molecular approaches, in *Organic Geochemistry: Principles and Applications*, pp. 185-210, edited by M.H. Engel and S.A. Macko, Plenum, New York, 1993.

Mariotti, A., J.C. Germon, P. Hubert, P. Kaiser, R. Letolle, A. Tardieux and P. Tardieux, Experimental determination of nitrogen kinetic isotope fractionation: Some principles; illustration for the denitrification and nitrification processes, *Plant and Soil, 62*, 413-430, 1981.

Martinson, D.G., Evolution of the Southern Ocean winter mixed layer and sea ice: Open ocean deep water formation and ventilation, *J. Geophys. Res., 95*, 11,641-11.654, 1990.

Mayer, L., Surface area control of organic carbon accumulation in continental shelf sediments, *Geochim. Cosmochim. Acta, 58*, 1271-1284, 1994.

Montoya, J.P. and J.J. McCarthy, Isotopic fractionation during nitrate uptake by marine phytoplankton grown in continuous culture, *J. Plankton Res., 17*, 439-464, 1995.

Morley, J.J. and J.D. Hays, Oceanographic conditions associated with high abundances of the radiolarian, *Cycladophora davisiana*, *Earth Planet. Sci. Lett., 66*, 63-72, 1983.

Muller, P.J., C/N ratios in Pacific deep-sea sediments: Effect of inorganic ammonium and organic nitrogen compounds sorbed by clays, *Geochim. Cosmochim. Acta, 41*, 765-776, 1977.

Nakatsuka, T., N. Handa, E. Wada, and C.S. Wong, The dynamic changes of stable isotope ratios of carbon and nitrogen in suspended and sedimented particulate organic matter during a phytoplankton bloom, *J. Mar. Res., 50*, 267-296, 1992.

Oppo, D.W. and R.G. Fairbanks, Variability in the deep and intermediate water circulation of the Atlantic Ocean during the past 25,000 years: Northern hemisphere modulation of the Southern Ocean, *Earth Planet. Sci. Lett., 86*, 1-15, 1987.

Orsi, A.H., T.W. Whitworth, and W.D. Nowlin, On the meridional extent and fronts of the Antarctic Circumpolar Current, *Deep Sea Res. Part I, 42*, 641-673, 1995.

Park, Y.-H. and L. Gamberoni, Cross-frontal exchange of Antarctic Intermediate Water and Antarctic Bottom Water in the Crozet Basin, *Deep Sea Res. Part II, 44*, 987-1004, 1997.

Pennock, J.R., D.J. Velinsky, D.J. Ludlam, J.H. Sharp, and M.L. Fogel, Isotopic fractionation of ammonium and nitrate during uptake by *Skeletonema costatum*: Implications for $\delta^{15}N$ dynamics under bloom conditions, *Limnol. Oceanogr., 41*, 451-459, 1996.

Riaux-Gobin, C., P.E. Hargraves, J. Neveux, L. Oriol, and G. Vetion, Microphyte pigments and resting spores at the water-sediment interface in the Subantarctic deep sea (Indian sector of the Southern Ocean), *Deep Sea Res. Part II, 44*, 1033-1052, 1997.

Sachs, J.P., Nitrogen isotopes in chlorophyll and the origin of the eastern Mediterranean sapropels, Ph.D. thesis, Mass. Inst. Technol./Woods Hole Oceanogr. Inst. Joint Program in Oceanography, Woods Hole, 1997.

Sarmiento, J.L. and J.C. Orr, Three-dimensional simulations of the impact of Southern Ocean nutrient depletion on atmospheric CO_2 and ocean chemistry, *Limnol Oceanogr., 36*, 1928-1950, 1991.

Sarmiento, J.L. and J.R. Toggweiler, A new model for the role of the oceans in determining atmospheric pCO_2, *Nature, 308*, 621-624, 1984.

Schrag, D.P. and D.J. DePaolo, Determination of d18O of seawater in the deep ocean during the last glacial maximum, *Paleoceanography, 8*, 1-6, 1993.

Senftle, J.T., C.R. Landis, and R. McLaughlin, Organic petrographic approach to kerogen characterization, in *Organic Geochemistry: Principles and Applications*, pp. 355-376, edited by M.H. Engel and S.A. Macko, Plenum, New York, 1993.

Shemesh, A., R.A. Mortlock, R.J. Smith, and P.N. Froelich, Determination of Ge/Si in marine siliceous microfossils: separation, cleaning and dissolution of diatoms and radiolaria, *Mar. Chem., 25*, 305-323, 1988.

Shemesh, A., S.A. Macko, C.D. Charles, G.H. Rau, Isotopic evidence for reduced productivity in the glacial Southern Ocean, *Science, 262*, 407-410, 1993.

Sieganthaler, U. and T. Wenk, Rapid atmospheric CO_2 variations and ocean circulation, *Nature, 308*, 624-626, 1984.

Sigman, D.M., The role of biological production in Pleistocene atmospheric carbon dioxide variations and the nitrogen isotope dynamics of the Southern Ocean, Ph.D. thesis, Mass. Inst. Technol./Woods Hole Oceanogr. Inst. Joint Program in Oceanography, Woods Hole, 1997.

Sigman, D.M., D.C. McCorkle, and W.R. Martin, The calcite lysocline as a constraint on glacial/interglacial low latitude production changes, *Global Biogeochem. Cycles, 12*, 409-428, 1998.

Singer, A.J. and A. Shemesh, Climatically linked carbon isotope variation during the past 430,000 years in Southern Ocean sediments, *Paleoceanography, 10*, 171-178, 1995.

Swift, D.M. and A.P. Wheeler, Evidence of an organic matrix from diatom biosilica, *J. Phycol., 28*, 202-209, 1992.

Talbot, V. and M. Bianchi, Bacterial proteolytic activity in sediments of the Subantarctic Indian Ocean sector, *Deep Sea Res. Part II, 44*, 1069-1084, 1997.

Toggweiler, J.R., and B. Samuels, Effect of Drake Passage on the global thermohaline circulation, *Deep Sea Res. Part I, 42*, 477-500, 1995.

Wada, E., Nitrogen isotope fractionation and its significance in biogeochemical processes occurring in marine environments, *Isotope Marine Chemistry*, edited by E. Goldberg, Y. Horibe and K. Saruhashi, pp. 375-398, Uchida Rokakuho, Tokyo, 1980.

Wada, E. and A. Hattori, Nitrogen isotope effects in the assimilation of inorganic nitrogenous compounds, *Geomicrobiol. J.*, *1*, 85-101, 1978.

Wada, E., M. Terazaki, Y. Kabaya, and T. Nemoto, ^{15}N and ^{13}C abundances in the Antarctic Ocean with emphasis on the biogeochemical structure of the food web, *Deep Sea Res. Part I*, *34*, 829-841, 1987.

Waser, N.A.D., D.H. Turpin, P.J. Harrison, B. Nielsen, and S.E. Calvert, Nitrogen isotope fractionation during the uptake and assimilation of nitrate, nitrite, and urea by a marine diatom, *Limnol. Oceanogr.*, *43* , 215-224, 1998.

Wu, J., S.E. Calvert, and C.S. Wong, Nitrogen isotope variations in the northeast subarctic Pacific: Relationships to nitrate utilization and trophic structure, *Deep Sea Res. Part I*, *44*, 287-314, 1997.

M.A. Altabet, Center for Marine Science and Technology, University of Massachusetts, New Bedford, MA 02744.

R. Francois and D.C. McCorkle, Department of Marine Chemistry and Geochemistry, Woods Hole Oceanographic Institution, Woods Hole, MA 02543.

J.F. Gaillard, Department of Geological Sciences, Northwestern University, Evanston, IL 60208.

D.M. Sigman, Department of Geosciences, Princeton University, Guyot Hall, Princeton, NJ 08544. (sigman@geo.princeton.edu)

(Received February 11, 1998;
revised November 5, 1998;
accepted November 13, 1998.)